
Collective Properties and Combined Quantum Transitions of Two-Dimensional Magnetoexcitons

S. A. MOSKALENKO,¹ M. A. LIBERMAN,² E. V. DUMANOV,¹
I. V. PODLESNY¹

¹*Institute of Applied Physics, Academy of Sciences of Moldova, Academic Str. 5, Chisinau, MD 2028, Republic of Moldova*

²*Department of Physics, Uppsala University, Box 530, SE-751 21, Uppsala, Sweden*

Received 6 November 2008; accepted 16 April 2009

Published online 13 August 2009 in Wiley InterScience (www.interscience.wiley.com).

DOI 10.1002/qua.22315

ABSTRACT: The article consists of two parts describing two associated properties of two-dimensional magnetoexcitons. In the first part, the theory of combined exciton-cyclotron resonance in the quantum well structures is developed for a strong magnetic field. In the first part, we calculate the absorption band structure for optical quantum transitions with circularly polarized radiation creating a two-dimensional exciton and simultaneously exciting one of the resident electrons from the lowest to the first excited Landau level. In the second part, we discuss the collective elementary excitations of the system of two-dimensional magnetoexcitons in the ground state of Bose–Einstein condensation on the arbitrary wave vector $\vec{k} \neq 0$ in the Hartree–Fock approximation. The breaking of the gauge symmetry of the initial Hamiltonian was introduced following the idea proposed by Bogoliubov in his theory of quasi-averages. The energy spectrum of the collective elementary excitations is characterized by the interconnection of the exciton and plasmon branches. © 2009 Wiley Periodicals, Inc. *Int J Quantum Chem* 110: 177–194, 2010

Key words: magnetoexcitons; Bose-Einstein condensation; two-dimensional; quantum transition; collective properties

Correspondence to: E. V. Dumanov; e-mail: dum@phys.asm.md

Contract grant sponsor: Russian Foundation for Fundamental Research and Academy of Sciences of Moldova.

Contract grant number: 08.820.05.033RF.

Contract grant sponsor: U.S. Civilian Research and Development Foundation (CRDF).

Contract grant number: MYSSP-1401.

Contract grant sponsor: Moldavian Research and Development Association (MRDA).

Contract grant number: 08.819.05.07F.

Contract grant sponsor: Academy of Sciences of Moldova.

Contract grant number: 08.822.05.07F.

Contract grant sponsor: Wenner-Gren Foundation.

1. Introduction

Properties of atoms and excitons are dramatically changed in the strong magnetic fields, such that the distance between Landau levels $\hbar\omega_c$ exceeds the corresponding Rydberg energies R_y and the magnetic length $l = \sqrt{\hbar c/eH}$ is small compared to their Bohr radii [1, 2]. Even more interesting phenomena are exhibited in the case of two-dimensional (2D) electron systems due to the quenching of the kinetic energy at high magnetic fields, with the representative example being integer and fractional quantum Hall effects (FQHE) [3–5]. The discovery of the FQHE [6–8] changed drastically the established concepts about charged elementary excitations in solids [5]. The notion of the incompressible quantum liquid (IQL) was introduced in Ref. [7] as a homogeneous phase with the quantized densities $\nu = p/q$, where p is an integer and $q \neq 1$ is odd having charged elementary excitations with a fractional charge $e^* = \pm e/q$. These quasiparticles were named *anyons*. A classification of free anyons and their hierarchy were studied in [9, 10]. An alternative concept to hierarchical scheme was proposed in [11], where the notion of the composite fermions (CF) was introduced. The CF consists of an electron bound to even number of flux quanta. In the frame of this concept the FQHE of the electrons can be understood as a manifestation of the integer quantum Hall effect (IQHE) of CFs [11]. The statistics of anyons was determined in [10, 12]. It was established that the wave function of the system changes by a complex phase factor $\exp[i\pi\alpha]$, when the quasiparticles are interchanged. For bosons, $\alpha = 0$, for fermions $\alpha = 1$ and for anyons with $e^* = -e/3$ their statistical charge is $\alpha = -1/3$. As was shown in Ref. [13] there are no soft branches of neutral excitations in IQL. The energy gap Δ for formation of quasielectron-quasihole pair has the scale of Coulomb energy $E_Q = e^2/\epsilon l$, where ϵ is the background dielectric constant. However, the energy gap was found to be small $\Delta \approx 0.1E_Q$. The lowest branch was called magnetoroton [13] and can be modeled as a quasiexciton [5]. As mentioned in [5], the traditional methods and the concepts based either on the neglecting by the electron-electron interaction or on self-consistent approximation are inapplicable to IQL. In a strong magnetic field, the binding energy of an exciton increases from R_y to I_l .

There are two another small parameters in the theory. One of them determines how strong the magnetic field strength H is, and it verifies whether the starting supposition of a strong magnetic field is fulfilled. This parameter is expressed by the ratio $I_l/\hbar\omega_c < 1$, where I_l is the magnetoexciton ionization potential, $I_l = e^2(\sqrt{\pi}/2)/(\epsilon l)$ and ω_c is the cyclotron frequency $eH/\mu c$ calculated with the reduced mass μ . Another small parameter has a completely different origin and it is related to the concentration of the electron-holes (e-h) pairs. In our case it can be expressed as a product of the filling factor $\nu = v^2$ and $(1 - v^2)$, which reflects the Pauli exclusion principle and the phase-space filing (PSF) effect. The parameter $v^2(1 - v^2)$ in the case of the Bose–Einstein condensed excitons can take the form u^2v^2 , where u, v are Bogoliubov transformation coefficients and $u^2 = (1 - v^2)$. But in the case of FQHE the filling factor $\nu = v^2$ basically determines the underlying physics and can not be changed arbitrarily. Instead of the perturbation theory based on the filling factor ν , the exact numerical diagonalization for a few number of particles $N \leq 10$ proved to be the most powerful tool for the studying such systems [5]. The spherical geometry for these calculations was proposed [10, 14], considering a few number of particles on the surface of a sphere with the radius $R = \sqrt{Sl}$, whereas S is the dimensional Haldane parameter, so as the density of the particles on the sphere to be equal the filling factor of 2DEG. The magnetic monopole in the center of the sphere creates a magnetic flux through the sphere $2S\phi_0$, which is multiple to the flux quantum $\phi_0 = 2\pi\hbar c/e$. The angular momentum L of the quantum state on the sphere and the quasimomentum k of the FQHE state on the plane obey the relation $L = Rk$. Spherical model is characterized by continuous rotational group, which is analogous with the continuous translational symmetry in the plane.

Properties of the symmetric 2D electron-hole (e-h) system, with equal concentrations of both components, with coincident matrix elements of Coulomb electron-electron, hole-hole, and electron-hole interactions in a strong perpendicular magnetic field also attracted a great attention during past two decades [15–22]. A hidden symmetry and the multiplicative states were discussed in the papers [19, 23, 24]. The collective states such as the Bose–Einstein condensation (BEC) of two-dimensional magnetoexcitons and the formation of the metallic-type electron-hole liquid (EHL) were in-

vestigated in [15–22]. The search for the Bose-Einstein condensate has become a milestone in the condensed matter physics [25]. The remarkable properties of superfluids and superconductors are intimately related to the existence of a bosonic condensate of the composite particles consisting of an even number of fermions. In highly excited semiconductors the role of such composite bosons is taken by excitons, which are bound states of electrons and holes. Furthermore, the excitonic system has been viewed as a keystone system for exploration of the BEC phenomena, since it allows to control particle densities and interactions in situ. Promising candidates for experimental realization of such a system are semiconductor quantum wells (QWs) [26], which have a number of advantages compared to the bulk systems. The coherent pairing of electrons and holes occupying only the lowest Landau levels (LLs) was studied using the Keldysh–Kozlov–Kopaev method and the generalized random-phase approximation in [20, 27]. The BEC of magnetoexcitons takes place on a single exciton state with wave vector k , supposing that the high density of electrons in the conduction band and of holes in the valence band were created in a single QW structure with size quantization much greater than the Landau quantization. In the case $k \neq 0$ a new metastable dielectric liquid phase formed by the Bose–Einstein condensed magnetoexcitons was revealed in [20, 21]. The authors of [16–19] first took into account importance of the excited Landau levels (ELs) and their influence on the ground states of the systems. The influence of the excited Landau levels (ELs) of electrons and holes was discussed in details in [21, 22]. The indirect attraction between electrons (e-e), between holes (h-h) and between electrons and holes (e-h) due to the virtual simultaneous quantum transitions of the interacting charges from LLs to the ELs is a result of their Coulomb scattering. The first step of the scattering and the return back to the initial states were described in the second order of the perturbation theory.

At the same time the ELs play an important role in the fundamental many body elementary and combined processes displayed in optical spectra such as shakeup processes [28, 29], where e-h pair recombination is accompanied by transition of the second electron to a higher energy state. A closely related phenomenon of combined exciton-cyclotron resonance (ExCR) was discovered in low-density 2DEG system of a semiconductor quantum well heterostructure [3, 4]. Here, an incident photon creates a Wannier–Mott exciton and simultaneously excites one of the resident electrons from the lowest

to a higher Landau level (LL). The ExCR line shifts linearly with the magnetic field strength with a slope comparable to the electron cyclotron frequency. The intensity of the ExCR line increases for higher illumination intensity, i.e., for larger $n_{el}(p)$, whereas the exciton lines remain insensitive. It was found [30, 31], that the ExCR line is strongly σ polarized. Influence of the magnetic field and Coulomb interaction on the combined ExCR was considered in different theoretical descriptions [30–32] based on the first order perturbation theory of the electron-photon interaction. In this article, we present a rigorous theory of the ExCR on the base of the second-order perturbation theory using as perturbations the electron-radiation interaction and the electron-electron Coulomb interaction.

According to [30, 31] the incident photon creates an electron-hole pair with different Landau quantum numbers n_e and n_h , so that the optically created hole with $n_e = 0$ together with the background electron in the initial state with $n_h = 0$ form the magnetoexciton $X_{0,0}$, whereas the optically created electron with $n_e = 1$ becomes a background electron in the final state with the same quantum number. In semiconductor quantum well structure of the type CdTe, the electrons belong to s-type conduction band with spin projections $s_z = \pm 1$, whereas the heavy-holes are formed in p-type valence band with orbital momentum projection $M = \pm 1$. The heavy holes with total momentum projections $j_z = \mp 3/2$ and electrons with spin projection $s_z = \pm 1/2$ form electron-hole pairs with $F = s_z + j_z = \mp 1$ coinciding with the orbital quantum number M . Without a magnetic field the band-to-band quantum transitions are of allowed type whereas in the presence of a strong perpendicular magnetic field they are dipole active when the created e-h pair has the same Landau quantum numbers $n_e = n_h$ and are quadrupole-active when the quantum numbers differ by 1, i.e. $n_e = n_h \pm 1$. In the later case, as will be shown below, the probability of quantum transition is proportional to $|\tilde{Q}_{2D}|^2$, where \tilde{Q}_{2D} is the projection of the light wave vector \tilde{Q} on the layer surface, which vanishes in the Faraday geometry of excitation.

2. Two-Dimensional Combined Magnetoexciton-Cyclotron Resonances in a Strong Magnetic Field

As mentioned earlier, we consider a strong magnetic field such that the distance between the

Landau levels is larger than the exciton Rydberg and the magnetic length $l = \sqrt{\hbar c/eH}$ is smaller than the Bohr radius $a_B = \epsilon\hbar^2/mc^2$, otherwise assuming small concentration of the resident electrons, which does not influence structure of the magnetoexcitons [30–33]. Let the light with a given circular polarization $\vec{\sigma}_Q$ creates an electron-heavy-hole pair with equal Landau quantum numbers $n_e = n_h = 0$ and circular polarization $\vec{\sigma}_M$ in the presence of a background electron. The amplitude of this matrix element is proportional to $(\vec{\sigma}_Q^* \cdot \vec{\sigma}_M)$ and depends essentially on the reciprocal spin orientations of the optically created electron defined by the value M and background electron. On the second step of the perturbation theory these two electrons undergo the Coulomb scattering process, and as a result one of them remains on the lowest Landau level and the second electron is transferred on the final state $n_e = 1$. Because the Coulomb direct and exchange interactions this scattering process depends on the mutual spin orientations of two electrons.

The probability of the transitions between the initial and the final states is

$$P(\omega_Q; i; F) = \frac{2\pi}{\hbar} |Z(i|F)|^2 \delta(E_i - E_F) \quad (1)$$

where the second-order matrix elements

$$Z(i|F) = \sum_u \frac{\langle i|H_{e\text{-rad}}|u\rangle \langle u|H_{\text{Coul}}|F\rangle}{E_i - E_u} \quad (2)$$

is calculated using the first-order matrix elements $\langle i|H_{e\text{-rad}}|u\rangle$ and $\langle u|H_{\text{Coul}}|F\rangle$ between the initial and intermediate and the final states. $H_{e\text{-rad}}$ is the Hamiltonian of electron-photon interaction describing only the band-to-band optical transitions, and H_{Coul} is the Hamiltonian of the electron-electron Coulomb interaction. E_i and E_u are energies of the initial and intermediate states. In the initial state there are a photon and a background electron described by the wave function

$$|i, \pm; \uparrow, 0, T\rangle = (C_{\vec{Q}\pm})^\dagger a_{1/2,0,T}^\dagger |0\rangle. \quad (3)$$

Here $(C_{\vec{Q}\pm})^\dagger = 1/\sqrt{2}(C_{\vec{Q},1} \pm iC_{\vec{Q},2})^\dagger$ is the photon creation operator with wave vector \vec{Q} , and circular polarization $(\vec{\sigma}_{\vec{Q}}^\pm)^* = 1/\sqrt{2}(\vec{e}_{\vec{Q},1} \mp i\vec{e}_{\vec{Q},2})^*$, where $\vec{e}_{\vec{Q},1}$ are the transverse linear polarizations. $a_{1/2,0,T}^\dagger$ is the electron creation operator labeled in Landau gauge

by the spin index $1/2$, quantum number $n_e = 0$, and unidimensional vector T .

The intermediate state $|u\rangle$ consists of the electron-heavy-hole pair with $n_e = n_h = 0$, wave numbers f and g , with spin and full momentum projections $s_z = \pm 1/2$, $j_z = \mp 3/2$ resulting in $M = \mp 1$ and circular polarization $\vec{\sigma}_M$ correspondingly, as well as of the background electron in the same initial state but with changed wave number h . Introducing the hole creation operator $b_{j_z, m_h, g}^\dagger$ the intermediate state can be written as

$$|u, \mp, \uparrow\rangle = |u, \mp, f, g; \uparrow, 0, h\rangle = a_{\pm 1/2, 2, 0, f}^\dagger b_{\mp 3/2, 2, 0, g}^\dagger a_{1/2, 2, 0, h}^\dagger |0\rangle \quad (4)$$

The final state $|F\rangle$ is the optically created magnetoexciton on the lowest Landau levels $n_e = n_h = 0$, with two-dimensional wave vector $\vec{k}_{\text{ex}} = (k_x, k_y)$ and the summary spin projection of the e-h pair $F = s_z + j_z = M = \mp 1$, together with the excited background electron on the state $n_e = 1$ with wave number R

$$|F, \vec{k}_{\text{ex}}, \pm; \uparrow, 1, R\rangle = \hat{\Psi}_{\text{ex}}^{(0,0)\dagger}(\vec{k}_{\text{ex}}, \pm) a_{1/2, 1, R}^\dagger |0\rangle, \quad (5)$$

where the exciton creation operator in Landau gauge [7, 8] is

$$\Psi_{\text{ex}}^{(n,m)\dagger}(\vec{k}, M = \pm 1) = \frac{1}{\sqrt{N}} \sum_t e^{iky} a_{\mp 1/2, n, \frac{k_x}{2} + t}^\dagger b_{\pm 3/2, m, \frac{k_x}{2} - t}^\dagger. \quad (6)$$

The creation energy of the magnetoexciton is

$$E_{\text{ex}}^{(n,m)}(\vec{k}, s_z, j_z) = E_g + \frac{1}{2}\hbar\omega_{c\mu} + n\hbar\omega_{ce} + m\hbar\omega_{ch} - I_{\text{ex}}^{(n,m)}(\vec{k}) + (g_e s_z + \tilde{g}_h j_z) \mu_B H, \quad (7)$$

where ω_{ce} , ω_{ch} , and $\omega_{c\mu}$ are the cyclotron frequencies for m_e , m_h and $\mu = m_e m_h / m_e + m_h$, $I_{\text{ex}}^{(n,m)}(k)$ is the ionization potential of magnetoexciton [34]. The last term, being the Zeeman energy, contains the g -factors \tilde{g}_e and \tilde{g}_h , which must be determined experimentally.

The full probability of the transition is obtained by summarizing (1) over T , multiplied by the filling factor ν^2 and summarizing over the quantum numbers \vec{k}_{ex} and R of the final states

$$W = \frac{\nu^2 S}{(2\pi)^2} \sum_T \sum_R \int d^2 \vec{k} P(\omega_Q; i; F) \quad (8)$$

To calculate the probability of the transitions, we use the matrix elements of the electron-photon interaction between the initial and the intermediate states expressed in the terms of the matrix element of the band-to-band transition $P_{cv}(\vec{k}, g)$ obtained in [35], and matrix elements of the electron-electron Coulomb interaction obtained in [34]. The later do not vanish only between the intermediate and final states with the same quantum number M because the light is not involved and does not influence symmetry of the 2D layer. For the background electrons polarized in the same direction as the direction of the magnetic field, $s_z = 1/2$ we obtain the probabilities of the quantum transition

$$W(\omega_Q; -; -; \uparrow) = \frac{8\pi\nu^2}{Ll_0^2} I_1 B(\omega_Q, -) \times \int_0^\infty x dx e^{-x^2} \left\{ \frac{1}{\pi} + \frac{x^2}{8} \left| {}_1F_1\left(\frac{1}{2}, 2, \frac{x^2}{2}\right) \right|^2 \right\} \times \delta\left(\tilde{\Delta}_- + e^{-\frac{x^2}{4}} I_0\left(\frac{x^2}{4}\right)\right), \quad (9)$$

where ${}_1F_1(a, b, x)$ is the confluent hypergeometric function [36].

For another circular polarization in the presence of the same background electrons

$$W(\omega_Q; +; +; \uparrow) = \frac{2\pi\nu^2}{Ll_0^2} I_1 B(\omega, +) \times \int_0^\infty x dx e^{-x^2} \delta\left(\tilde{\Delta}_+ + e^{-\frac{x^2}{4}} I_0\left(\frac{x^2}{4}\right)\right). \quad (10)$$

For two other configurations the probabilities of transitions vanish

$$W(\omega_Q; -; +; \uparrow) = W(\omega_Q; +; -; \uparrow) = 0 \quad (11)$$

Here $x = kl$ and $\tilde{\Delta}_\pm = \Delta_\pm / I_l$ are the dimensionless wave vector and the energy detuning, $I_{\text{ex}}^{(0,0)}(k) = e^{-x^2/4} I_0(x^2/4)$ is the magnetoexciton ionization potential, $I_0(z)$ is the modified Bessel function, and $B(\omega_Q, \pm)$ is expressed following to [35] in the matrix element of the band-to-band transition $P_{cv}(\vec{k}, g)$

$$B(\omega_Q, \pm) = \frac{\left(\frac{e}{m_0}\right)^2 |P_{cv}|^2}{\omega_Q \left[\hbar\omega_Q - E_g - \frac{1}{2} \hbar\omega_{cm} \mp \left(\frac{3}{2} g_h - \frac{1}{2} g_e\right) \mu_B H \right]^2} \quad (12)$$

The probabilities of quantum transitions depend on the reciprocal orientation of the photon and exciton circular polarization vectors $\vec{\sigma}_k^\pm$ and $\vec{\sigma}_M$ expressed by the factor $|(\vec{\sigma}_k^\pm \cdot \vec{\sigma}_M)|^2$. In the Faraday geometry light propagates along the magnetic field, $Q_{2D} = 0$ and $\vec{\sigma}_Q^\pm$ coincides with $\vec{\sigma}_M$, so that $\vec{\sigma}_Q^+ = \vec{\sigma}_1$ and $\vec{\sigma}_Q^- = \vec{\sigma}_{-1}$. This means spin polarization of the e-h pair because the magnetoexciton with $M = -1$ is composed of the heavy-hole with $j_z = -3/2$ and electron with $s_z = 1/2$ whereas the magnetoexciton with $M = +1$ is composed of the heavy-hole with $j_z = 3/2$ and electron with $s_z = -1/2$. Two electrons with $s_z = 1/2$ in the intermediate state interdependently participate in the quantum transition being identical, so that a direct and exchange terms are involved. On the contrary, two electrons with different spins participate separately in the transition. This difference essentially influences probability of the combined quantum transition, which is expressed in additional factor 4 in the expression (9) with participation of two electrons with parallel spins compared to the probability with participation of two electrons with antiparallel spin projections. The transition probability is strongly enhanced if the circularly polarized light excites an e-h pair so that the electron polarization of the magnetoexciton and of the background electrons are the same.

The momentum conservation for the magnetoexciton-photon quantum transition is implemented by the equality $\vec{k}_{\text{ex}} = \vec{Q}_{2D}$, whereas the combined quantum transition is governed by the conservation law for only one component of the involved momenta. It reflects the symmetry properties of 2D e-h system in a strong magnetic field [32, 33, 37].

The expressions (9–12) describe the dipole-active quantum transitions, providing full description of the probabilities of the combined quantum transitions. The coefficients $B(\omega_Q, \pm)$ together with integrals in (9, 10) determine the band shapes in the whole energy intervals of the absorption bands, $-1 \leq \tilde{\Delta}_\pm \leq 0$. The analytical expressions for the band shapes can be obtained [35] in the vicinities of the band edges, at $\tilde{\Delta}_+ \approx 0$ and $\tilde{\Delta}_+ \approx -1$.

Spectral functions $f_1(\tilde{\Delta})$ and $f_2(\tilde{\Delta})$ corresponding to the integrals in (9, 10) determining the absorption band shapes for two circular light polarizations in

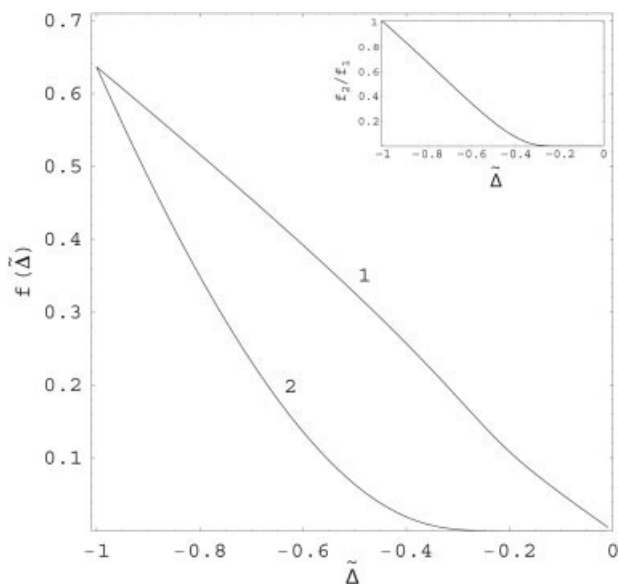


FIGURE 1. The absorption band shapes for two circular polarizations of the light in the Faraday geometry: $f_1(\tilde{\Delta})$ — curve 1, $f_2(\tilde{\Delta})$ — curve 2. The ratio of f_2/f_1 is shown in the inset.

the Faraday geometry are depicted in Figure 1. Both spectral functions have the same maximal spectral width corresponding to the ionization potential I_i of the magnetoexciton $X_{0,0}$ at $k = 0$ (unity in nondimensional energy units). This means that all points of the magnetoexciton band take part in the quantum transition due to participation of the background electrons. The maximum width of the band shapes is the same for both circular polarizations because this feature is exclusively due to the momentum conservation law in x in-plane direction in the Landau gauge description. Both functions $f_1(\tilde{\Delta})$ and $f_2(\tilde{\Delta})$ decrease linearly near $\tilde{\Delta} = -1$ but $f_1(\tilde{\Delta})$ decreases with a smaller slope than $f_2(\tilde{\Delta})$. In the vicinity of $\tilde{\Delta} = 0$ $f_1(\tilde{\Delta})$ vanishes linearly due to exclusively the exchange Coulomb interaction term, while $f_2(\tilde{\Delta})$ has an exponentially decreasing tail.

Similar to [34] these calculations are valid in the range of magnetic field, where the electron cyclotron energy exceeds the value of the ionization potential $I_i(H)$.

3. Collective Elementary Excitations of Two-Dimensional Magnetoexcitons in the Bose-Einstein Condensation State

For the very beginning we will introduce the operators describing the magneto-excitations and plasmons, and their commutation relations.

The creation and annihilation operators of magnetoexcitons are two-particle operators reflecting the electron-hole (e-h) structure of the excitons. They are denoted below as $d^+(\vec{P})$ and $d(\vec{P})$, where $\vec{P}(p_x, p_y)$ is the two-dimensional wave vector. There are also the density fluctuation operators for electrons $\hat{\rho}_e(\vec{Q})$ and for holes $\hat{\rho}_h(\vec{Q})$ as well as their linear combinations $\hat{\rho}(\vec{Q})$ and $\hat{D}(\vec{Q})$. They are determined below

$$\hat{\rho}_e(\vec{Q}) = \sum_t e^{iQ_y t l^2} a_{t-\frac{Q_x}{2}}^\dagger a_{t+\frac{Q_x}{2}},$$

$$\hat{\rho}_h(\vec{Q}) = \sum_t e^{iQ_y t l^2} a_{t+\frac{Q_x}{2}}^\dagger a_{t-\frac{Q_x}{2}},$$

$$\hat{\rho}(\vec{Q}) = \hat{\rho}_e(\vec{Q}) - \hat{\rho}_h(-\vec{Q});$$

$$\hat{D}(\vec{Q}) = \hat{\rho}_e(\vec{Q}) + \hat{\rho}_h(-\vec{Q});$$

$$d^+(\vec{P}) = \frac{1}{\sqrt{N}} \sum_t e^{-iP_y t l^2} a_{t+\frac{P_x}{2}}^\dagger b_{-t+\frac{P_x}{2}},$$

$$d(\vec{P}) = \frac{1}{\sqrt{N}} \sum_t e^{iP_y t l^2} b_{-t+\frac{P_x}{2}} a_{t+\frac{P_x}{2}},$$

$$\hat{N}_e = \hat{\rho}_e(0);$$

$$\hat{N}_h = \hat{\rho}_h(0);$$

$$\hat{\rho}(0) = \hat{N}_e - \hat{N}_h;$$

$$\hat{D}(0) = \hat{N}_e + \hat{N}_h; \quad (14)$$

and are expressed through the Fermi creation and annihilation operators $a_{p_x}^\dagger, a_{p_x}$ for electrons and $b_{p_x}^\dagger, b_{p_x}$ for holes. The e-h Fermi operators depend on two quantum numbers. In Landau gauge one of them is the wave number p and the second one is the quantum number n of the Landau level. In the lowest Landau level (LLL) approximation n has only the value zero and its notation is dropped. The wave number p enumerates the N -fold degenerate states of the 2D electrons in a strong magnetic field. N can be expressed through the layer surface area S and the magnetic length l as follows: $N = S/2\pi l^2$; $l^2 = \hbar c/eH$, where H is the magnetic field strength. The operators (14) obey to the following commutation relations, most of which were discussed for first time in the papers [5, 13]

$$[\hat{\rho}(\vec{Q}), \hat{\rho}(\vec{P})] = -2i \text{Sin} \left(\frac{[\vec{P} \times \vec{Q}]_z l^2}{2} \right) \hat{\rho}(\vec{P} + \vec{Q})$$

$$[\hat{D}(\vec{Q}), \hat{D}(\vec{P})] = -2i \text{Sin} \left(\frac{[\vec{P} \times \vec{Q}]_z l^2}{2} \right) \hat{\rho}(\vec{P} + \vec{Q})$$

$$[\hat{\rho}(\vec{Q}), \hat{D}(\vec{P})] = -2i \text{Sin}\left(\frac{[\vec{P} \times \vec{Q}]_z l^2}{2}\right) \hat{D}(\vec{P} + \vec{Q}) \quad (15)$$

$$[d(p), d^+(Q)] = \delta_{kr}(\vec{P}, \vec{Q}) - \frac{1}{N} \left[i \text{Sin}\left(\frac{[\vec{P} \times \vec{Q}]_z l^2}{2}\right) \hat{\rho}(\vec{P} - \vec{Q}) + \text{Cos}\left(\frac{[\vec{P} \times \vec{Q}]_z l^2}{2}\right) \hat{D}(\vec{P} - \vec{Q}) \right]$$

$$[\hat{\rho}(\vec{P}), d(\vec{Q})] = 2i \text{Sin}\left(\frac{[\vec{P} \times \vec{Q}]_z l^2}{2}\right) d(\vec{P} + \vec{Q})$$

$$[\hat{\rho}(\vec{P}), d^+(\vec{Q})] = -2i \text{Sin}\left(\frac{[\vec{P} \times \vec{Q}]_z l^2}{2}\right) d^+(-\vec{P} + \vec{Q})$$

$$[\hat{D}(\vec{P}), d^+(\vec{Q})] = 2 \text{Cos}\left(\frac{[\vec{P} \times \vec{Q}]_z l^2}{2}\right) d^+(\vec{Q} - \vec{P})$$

$$[\hat{D}(\vec{P}), d(\vec{Q})] = -2 \text{Cos}\left(\frac{[\vec{P} \times \vec{Q}]_z l^2}{2}\right) d(\vec{P} + \vec{Q}) \quad (16)$$

One can observe that the density fluctuation operators (14) with different wave vectors \vec{P} and \vec{Q} do not commute. Their noncommutativity is related with the vorticity which accompanies the presence of the strong magnetic field and depends on the vector-product of two wave vectors \vec{P} and \vec{Q} and its projection on the direction of the magnetic field $(\vec{P} \times \vec{Q})_z$. These properties considerably influence on the structure of the equations of motion for the operators (14) and determine new aspect of the magneto-exciton-plasmon physics. Indeed in the case of 3D e-h plasma in the absence of the external magnetic field the density fluctuation operators do

commute [38]. The magneto-exciton creation and annihilation operators $d^+(\vec{P})$ and $d^+(\vec{Q})$ as in general case do not obey exactly to the Bose commutation rule. Their deviation from it is proportional to the density fluctuation operators $\hat{\rho}(\vec{P} - \vec{Q})$ and $\hat{D}(\vec{P} - \vec{Q})$. The above discussed operators determine the structure of the 2D e-h system Hamiltonian in the LLL approximation. In the previous papers [16, 17, 19–21] the initial Hamiltonian was gauge-invariant.

It has the form

$$\hat{H} = \frac{1}{2} \sum_{\vec{Q}} W_{\vec{Q}} [\hat{\rho}(\vec{Q}) \hat{\rho}(-\vec{Q}) - \hat{N}_e - \hat{N}_h] - \mu_e \hat{N}_e - \mu_h \hat{N}_h \quad (17)$$

where

$$W_{\vec{Q}} = \frac{2\pi e^2}{\epsilon_0 S |\vec{Q}|} \text{Exp}\left[-\frac{Q^2 l^2}{2}\right]; \mu = \mu_e + \mu_h \quad (18)$$

The starting Hamiltonian \hat{H} in the quasiaverages theory approximation (QATA) has form

$$\hat{H} = \frac{1}{2} \sum_{\vec{Q}} W_{\vec{Q}} [\rho(\vec{Q}) \rho(-\vec{Q}) - \hat{N}_e - \hat{N}_h] - \mu_e \hat{N}_e - \mu_h \hat{N}_h - \eta \sqrt{N} (e^{i\varphi} d^+(k) - e^{i\varphi} d(k)) \quad (19)$$

The equations of motion for the operators (14) are obtained using the commutation relations (16). They are

$$i\hbar \frac{d}{dt} d(\vec{P}) = [d(\vec{P}), \hat{H}] = (E(\vec{P}) - \bar{\mu}) d(\vec{P}) - \eta \sqrt{N} e^{i\varphi} \delta_{kr}(\vec{P}, \vec{K}) - 2i \sum_{\vec{Q}} W_{\vec{Q}} \text{Sin}\left(\frac{[\vec{P} \times \vec{Q}]_z l^2}{2}\right) \hat{\rho}(\vec{Q}) d(\vec{P} - \vec{Q}) + \eta e^{i\varphi} \left[i \text{Sin}\left(\frac{[\vec{P} \times \vec{K}]_z l^2}{2}\right) \frac{\hat{\rho}(\vec{P} - \vec{K})}{\sqrt{N}} + \text{Cos}\left(\frac{[\vec{P} \times \vec{K}]_z l^2}{2}\right) \frac{\hat{D}(\vec{P} - \vec{K})}{\sqrt{N}} \right];$$

$$i\hbar \frac{d}{dt} d^+(2\vec{K} - \vec{P}) = [d^+(2\vec{K} - \vec{P}), \hat{H}] = (\bar{\mu} - E(2\vec{K} - \vec{P})) d^+(2\vec{K} - \vec{P}) + \eta \sqrt{N} e^{-i\varphi} \delta_{kr}(\vec{P}, \vec{K}) - 2i \sum_{\vec{Q}} W_{\vec{Q}} \text{Sin} \times \left(\frac{[(2\vec{K} - \vec{P}) \times \vec{Q}]_z l^2}{2} \right) \times d^+(2\vec{K} - \vec{P} - \vec{Q}) \hat{\rho}(-\vec{Q}) - \eta e^{-i\varphi} \times \left[i \text{Sin}\left(\frac{[\vec{P} \times \vec{K}]_z l^2}{2}\right) \frac{\hat{\rho}(\vec{P} - \vec{K})}{\sqrt{N}} + \text{Cos}\left(\frac{[\vec{P} \times \vec{K}]_z l^2}{2}\right) \frac{\hat{D}(\vec{P} - \vec{K})}{\sqrt{N}} \right];$$

$$\begin{aligned}
 i\hbar \frac{d}{dt} \hat{\rho}(\vec{P} - \vec{K}) &= [\hat{\rho}(\vec{P} - \vec{K}), \hat{H}] = -i \sum_{\vec{Q}} W_{\vec{Q}} \text{Sin} \left(\frac{[(\vec{P} - \vec{K}) \times \vec{Q}]_z L^2}{2} \right) [\hat{\rho}(\vec{P} - \vec{K} - \vec{Q}) \hat{\rho}(\vec{Q}) + \hat{\rho}(\vec{Q}) \hat{\rho}(\vec{P} - \vec{K} - \vec{Q})] \\
 &\quad - 2i\eta \sqrt{N} \text{Sin} \left(\frac{[(\vec{P} \times \vec{K})_z L^2]}{2} \right) \times [e^{-i\varphi} d(\vec{P}) - e^{i\varphi} d^\dagger(2\vec{K} - \vec{P})]; \\
 i\hbar \frac{d}{dt} \hat{D}(\vec{P} - \vec{K}) &= [\hat{D}(\vec{P} - \vec{K}), \hat{H}] = -i \sum_{\vec{Q}} W_{\vec{Q}} \text{Sin} \left(\frac{[(\vec{P} - \vec{K}) \times \vec{Q}]_z L^2}{2} \right) [\hat{\rho}(\vec{Q}) \hat{D}(\vec{P} - \vec{K} - \vec{Q}) + \hat{D}(\vec{P} - \vec{K} - \vec{Q}) \hat{\rho}(\vec{Q})] \\
 &\quad + 2\eta \sqrt{N} \text{Cos} \left(\frac{[(\vec{P} \times \vec{K})_z L^2]}{2} \right) [e^{-i\varphi} d(\vec{P}) - e^{i\varphi} d^\dagger(2\vec{K} - \vec{P})]. \quad (20)
 \end{aligned}$$

Here

$$\begin{aligned}
 \eta &= (E_{ex}(K) - \mu)v = (E(K) - \mu)v; \\
 v &= v^2; N_{ex} = v^2 N. \quad (21)
 \end{aligned}$$

Following the equations of motion (20) we will introduce four interconnected retarded Green's functions at $T = 0$ [39, 40]

$$\begin{aligned}
 G_{11}(\vec{P}, t) &= \langle \langle d(\vec{P}, t); d^\dagger(\vec{P}, 0) \rangle \rangle; \\
 G_{12}(\vec{P}, t) &= \langle \langle d^\dagger(2\vec{k} - \vec{P}, t); d^\dagger(\vec{P}, 0) \rangle \rangle; \\
 G_{13}(\vec{P}, t) &= \left\langle \left\langle \frac{\hat{\rho}(\vec{P} - \vec{k}, t)}{\sqrt{N}}; d^\dagger(\vec{P}, 0) \right\rangle \right\rangle; \\
 G_{14}(\vec{P}, t) &= \left\langle \left\langle \frac{\hat{D}(\vec{P} - \vec{k}, t)}{\sqrt{N}}; d^\dagger(\vec{P}, 0) \right\rangle \right\rangle. \quad (22)
 \end{aligned}$$

They are determined by the relations

$$\begin{aligned}
 G(t) &= \langle \langle \hat{A}(t); \hat{B}(0) \rangle \rangle = -i\theta[A(t), B(0)]; \\
 \hat{A}(t) &= e^{\frac{i\hbar t}{\hbar}} \hat{A} e^{-\frac{i\hbar t}{\hbar}}; \quad [\hat{A}, \hat{B}] = \hat{A}\hat{B} - \hat{B}\hat{A} \quad (23)
 \end{aligned}$$

where \hat{H} is the Hamiltonian (19).

The average $\langle \rangle$ will be calculated at $T = 0$ in HFB approximation using the ground state wave function $|\psi_g(k)\rangle$ (11). The time derivative of the Green's function is calculated as follows

$$\begin{aligned}
 i\hbar \frac{d}{dt} G(t) &= i\hbar \frac{d}{dt} \langle \langle A(t); B(0) \rangle \rangle = \hbar \delta(t) \langle [\hat{A}(0), \hat{B}(0)] \rangle \\
 &\quad + \left\langle \left\langle i\hbar \frac{d}{dt} A(t); B(0) \right\rangle \right\rangle = \hbar \delta(t) C \\
 &\quad + \langle \langle [\hat{A}(t), \hat{H}]; \hat{B}(0) \rangle \rangle \quad (24)
 \end{aligned}$$

By C will be denoted the average values, which do not depend on t . They are not needed in an explicit

form for the determination of the energy spectrum of the elementary excitations.

Fourier transforms of the Green's functions (29) will be denoted as

$$\begin{aligned}
 G_{11}(\vec{P}, \omega) &= \langle \langle d(\vec{P}) | d^\dagger(\vec{P}) \rangle \rangle_\omega; \\
 G_{12}(\vec{P}, \omega) &= \langle \langle d^\dagger(2\vec{k} - \vec{P}) | d^\dagger(\vec{P}) \rangle \rangle_\omega; \\
 G_{13}(\vec{P}, \omega) &= \left\langle \left\langle \frac{\hat{\rho}(\vec{P} - \vec{K})}{\sqrt{N}} \middle| d^\dagger(\vec{P}) \right\rangle \right\rangle_\omega; \\
 G_{14}(\vec{P}, \omega) &= \left\langle \left\langle \frac{\hat{D}(\vec{P} - \vec{K})}{\sqrt{N}} \middle| d^\dagger(\vec{P}) \right\rangle \right\rangle_\omega. \quad (25)
 \end{aligned}$$

The two representations are related to each other

$$G(\vec{P}, \omega) = \int_{-\infty}^{\infty} e^{i\omega t} G(\vec{P}, t) dt = \int_0^{\infty} e^{i\omega t - \delta t} G(\vec{P}, t) dt$$

where the infinitesimal value $\delta \rightarrow +0$ guarantees for the retarded Green's function $G(\vec{P}, t)$ the convergence of the integral in the interval $(0, \infty)$.

The equation of motion in the frequency representation can be deduced on the basis of Eq. (31)

$$\begin{aligned}
 \int_{-\infty}^{\infty} dt e^{i\omega t} i\hbar \frac{dG(t)}{dt} &= i\hbar \int_0^{\infty} dt e^{i\omega t - \delta t} \frac{dG(t)}{dt} = \\
 &= -i\hbar \int_0^{\infty} dt G(t) \frac{d e^{i\omega t - \delta t}}{dt} = (\hbar\omega + i\delta)G(\omega) = C \\
 &\quad + \int_{-\infty}^{\infty} dt \langle \langle [\hat{A}(t), \hat{H}]; \hat{B}(0) \rangle \rangle e^{i\omega t} \quad (26)
 \end{aligned}$$

The Green's functions (25) will be named as one-operator Green's functions because they contain in

the left-hand side of the vertical line only one summary operator of the types $d(P)$, $d^+(P)$, $\hat{\rho}(P)$, and $\hat{D}(P)$. At the same time these Green's functions are two-particle Green's functions, because the summary operators (14) are expressed through the products of two Fermi operators. In this sense the Green's functions (25) are equivalent with the two-particle Green's functions introduced by Keldysh and Kozlov in their fundamental paper [27], forming the base of the theory of high density excitons in the electron-hole description. But in difference on [27] we are using the summary operators (14), which represent integrals on the wave vectors of relative motions.

The equations of motion for the Green's function (25) are the following

$$[\hbar\omega + \bar{\mu} - E(\vec{P}) + i\delta]G_{11}(\vec{P}, \omega) = C - 2i \sum_{\vec{Q}} W_{\vec{Q}} \text{Sin} \left(\frac{[\vec{P} \times \vec{Q}]_z L^2}{2} \right) \langle \langle \hat{\rho}(\vec{Q}) d(\vec{P} - \vec{Q}) | d^+(\vec{P}) \rangle \rangle_{\omega} + \eta e^{i\varphi} \left[i \text{Sin} \left(\frac{[\vec{P} \times \vec{K}]_z L^2}{2} \right) G_{13}(\vec{P}, \omega) + \text{Cos} \left(\frac{[\vec{P} \times \vec{K}]_z L^2}{2} \right) G_{14}(\vec{P}, \omega) \right];$$

$$[\hbar\omega - \bar{\mu} + E(2\vec{K} - \vec{P}) + i\delta]G_{14}(\vec{P}, \omega) = C - 2i \sum_{\vec{Q}} W_{\vec{Q}} \text{Sin} \left(\frac{[(2\vec{K} - \vec{P}) \times \vec{Q}]_z L^2}{2} \right) \langle \langle d^+(2\vec{k} - \vec{P} - \vec{Q}) \hat{\rho}(-\vec{Q}) | d^+(\vec{P}) \rangle \rangle_{\omega} - \eta e^{-i\varphi} \left[i \text{Sin} \left(\frac{[\vec{P} \times \vec{K}]_z L^2}{2} \right) G_{13}(\vec{P}, \omega) + \text{Cos} \left(\frac{[\vec{P} \times \vec{K}]_z L^2}{2} \right) G_{14}(\vec{P}, \omega) \right];$$

$$[\hbar\omega + i\delta]G_{13}(\vec{P}, \omega) = C - i \sum_{\vec{Q}} W_{\vec{Q}} \text{Sin} \left(\frac{[(\vec{P} - \vec{K}) \times \vec{Q}]_z L^2}{2} \right) \times \left\langle \left\langle \left[\frac{\hat{\rho}(\vec{P} - \vec{K} - \vec{Q})}{\sqrt{N}} \hat{\rho}(\vec{Q}) + \hat{\rho}(\vec{Q}) \frac{\hat{\rho}(\vec{P} - \vec{K} - \vec{Q})}{\sqrt{N}} \right] \right\rangle \right\rangle \times d^+(\vec{P}) \Bigg\rangle_{\omega} - 2i\eta \text{Sin} \left(\frac{[\vec{P} \times \vec{K}]_z L^2}{2} \right) [e^{-i\varphi} G_{11}(\vec{P}, \omega) - e^{i\varphi} G_{12}(\vec{P}, \omega)];$$

$$[\hbar\omega + i\delta]G_{14}(\vec{P}, \omega) = C - i \sum_{\vec{Q}} W_{\vec{Q}} \text{Sin} \left(\frac{[(\vec{P} - \vec{K}) \times \vec{Q}]_z L^2}{2} \right) \left\langle \left\langle \left[\hat{\rho}(\vec{Q}) \frac{\hat{D}(\vec{P} - \vec{K} - \vec{Q})}{\sqrt{N}} \right] \right\rangle \right\rangle$$

$$+ \frac{\hat{D}(\vec{P} - \vec{K} - \vec{Q})}{\sqrt{N}} \hat{\rho}(\vec{Q}) \Bigg] \Bigg\rangle_{\omega} + 2\eta \text{Cos} \left(\frac{[\vec{P} \times \vec{K}]_z L^2}{2} \right) \times [e^{-i\varphi} G_{11}(\vec{P}, \omega) - e^{i\varphi} G_{12}(\vec{P}, \omega)]. \quad (27)$$

The equation of motion (27) for one-operator Green's functions $G_{1j}(\vec{P}, \omega)$, where $j = 1, 2, 3, 4$, give rise to new two-operator (four-particle) Green's functions of the types $\langle \langle \hat{P}(\vec{Q}) d(\vec{P} - \vec{Q}) | d^+(\vec{P}) \rangle \rangle_{\omega}$, $\langle \langle d^+(2\vec{k} - \vec{P} - \vec{Q}) \hat{\rho}(-\vec{Q}) | d^+(\vec{P}) \rangle \rangle_{\omega}$, $\langle \langle \hat{\rho}(\vec{P} - \vec{k} - \vec{Q}) \rho(\vec{Q}) / \sqrt{N}(\vec{Q}) | d^+(\vec{P}) \rangle \rangle_{\omega}$, and $\langle \langle \hat{D}(\vec{P} - \vec{k} - \vec{Q}) \rho(\vec{Q}) / \sqrt{N} \hat{\rho}(\vec{Q}) | d^+(\vec{P}) \rangle \rangle_{\omega}$ generated by the nonlinear terms in the equations of motion (24) for the operators (14). It is a well known situation described by Zubarev [40] in his review article. For these two-operator Green's functions of the first generation following the rule (26) the new equations of motion were deduced. This second step in the frame of the given method will form the second link of an infinite chain of equations of motion. Both links constructed in such a way will be exact in the frame of the Hamiltonian (19). These new equations of motion will contain in their components new types of three-operator Green's functions of the first generation as well as new types of the two-operator Green's functions of the second generation, and so on.

The interruption of these infinite chains of equations of motion is needed using reasonable approximations. Following the Zubarev's method [40] we will truncate the three-operator Green's functions expressing them through the one-operator Green's functions (25) multiplied by the average values of another two remaining operators. This method, if applied to the two-operator Green's functions of the second generation means in fact to linearize them.

The linearization can be achieved conserving only the macroscopic large values of the operators substituting them by their average values at some well definite values of the wave vector and neglecting all their infinitesimal values as follows

$$d(\vec{P}) \approx \delta_{kr}(\vec{P}, \vec{K}) e^{i\varphi} \sqrt{N_{ex}}; \quad d^+(\vec{P}) \approx \delta_{kr}(\vec{P}, \vec{K}) e^{-i\varphi} \sqrt{N_{ex}}; \\ \hat{D}(\vec{P}) \approx \delta_{kr}(\vec{P}, 0) \langle \hat{D}(0) \rangle \approx \delta_{kr}(\vec{P}, 0) 2N_{ex}; \\ \rho(\vec{P}) \approx \delta_{kr}(\vec{P}, 0) \langle \hat{\rho}(0) \rangle = 0. \quad (28)$$

The truncation procedure was successfully applied in the case of electron-phonon interaction not only for the metals in normal states but also for the superconductors.

It can be applied also in the case of Bose-Einstein condensed magnetoexcitons because this phenomenon was taken into account for the very beginning

by the Bogoliubov method of quasiaverages. The calculations of the average values of the products of two operators extracted from the left-hand side of the three-operator Green's functions have on made using the ground state wave function of the Bose-

Einstein condensed magnetoexcitons. On the basis of this some supplementary simplifications of the cumbersome expressions were proposed.

$G_{13}(\vec{P}, \omega)$ we will obtain

$$\begin{aligned}
 & -i \sum_{\vec{Q}} W_{\vec{Q}} \text{Sin} \left(\frac{[(\vec{P} - \vec{K}) \times \vec{Q}]_z L^2}{2} \right) \left\langle \left\langle \left[\frac{\hat{\rho}(\vec{P} - \vec{K} - \vec{Q})}{\sqrt{N}} \hat{\rho}(\vec{Q}) + \hat{\rho}(\vec{Q}) + \frac{\hat{\rho}(\vec{P} - \vec{K} - \vec{Q})}{\sqrt{N}} \right] d^+(\vec{P}) \right\rangle \right\rangle_{\omega} \\
 & = C - \frac{1}{(\hbar\omega + i\delta)} \sum_{\vec{Q}, \vec{R}} W_{\vec{Q}} W_{\vec{R}} \text{Sin} \left(\frac{[(\vec{P} - \vec{K}) \times \vec{Q}]_z L^2}{2} \right) \text{Sin} \left(\frac{[(\vec{P} - \vec{K} - \vec{Q}) \times \vec{K}]_z L^2}{2} \right) \\
 & \quad \times \left\langle \left\langle \left[\frac{\hat{\rho}(\vec{P} - \vec{K} - \vec{Q} - \vec{R})}{\sqrt{N}} \hat{\rho}(\vec{R}) \hat{\rho}(\vec{Q}) + \hat{\rho}(\vec{R}) \frac{\hat{\rho}(\vec{P} - \vec{K} - \vec{Q} - \vec{R})}{\sqrt{N}} \hat{\rho}(\vec{Q}) + \hat{\rho}(\vec{Q}) \frac{\hat{\rho}(\vec{P} - \vec{K} - \vec{Q} - \vec{R})}{\sqrt{N}} \hat{\rho}(\vec{R}) \right. \right. \\
 & \quad \left. \left. + \hat{\rho}(\vec{Q}) \hat{\rho}(\vec{R}) \frac{\hat{\rho}(\vec{P} - \vec{K} - \vec{Q} - \vec{R})}{\sqrt{N}} \right] d^+(\vec{P}) \right\rangle \right\rangle_{\omega} - \frac{1}{(\hbar\omega + i\delta)} \sum_{\vec{Q}, \vec{R}} W_{\vec{Q}} W_{\vec{R}} \text{Sin} \left(\frac{[(\vec{P} - \vec{K}) \times \vec{Q}]_z L^2}{2} \right) \text{Sin} \left(\frac{[\vec{Q} \times \vec{R}]_z L^2}{2} \right) \\
 & \quad \times \left\langle \left\langle \left[\frac{\hat{\rho}(\vec{P} - \vec{K} - \vec{Q})}{\sqrt{N}} \hat{\rho}(\vec{R}) \hat{\rho}(\vec{Q} - \vec{R}) + \frac{\hat{\rho}(\vec{P} - \vec{K} - \vec{Q})}{\sqrt{N}} \hat{\rho}(\vec{Q} - \vec{R}) \hat{\rho}(\vec{R}) + \hat{\rho}(\vec{R}) \hat{\rho}(\vec{Q} - \vec{R}) \frac{\hat{\rho}(\vec{P} - \vec{K} - \vec{Q})}{\sqrt{N}} \right. \right. \\
 & \quad \left. \left. + \hat{\rho}(\vec{Q} - \vec{R}) \hat{\rho}(\vec{R}) \frac{\hat{\rho}(\vec{P} - \vec{K} - \vec{Q})}{\sqrt{N}} \right] d^+(\vec{P}) \right\rangle \right\rangle_{\omega} - \frac{2\eta}{(\hbar\omega + i\delta)} \sum_{\vec{Q}} W_{\vec{Q}} \text{Sin} \left(\frac{[(\vec{P} - \vec{K}) \times \vec{Q}]_z L^2}{2} \right) \\
 & \quad \times \text{Sin} \left(\frac{[(\vec{P} - \vec{Q}) \times \vec{K}]_z L^2}{2} \right) [e^{-i\varphi} \langle \langle (d(\vec{P} - \vec{Q}) \hat{\rho}(\vec{Q}) + \hat{\rho}(\vec{Q}) d(\vec{P} - \vec{Q})) | d^+(\vec{P}) \rangle \rangle_{\omega} - e^{i\varphi} \langle \langle (d^+(2\vec{K} - \vec{P} + \vec{Q}) \hat{\rho}(\vec{Q}) \\
 & \quad + \hat{\rho}(\vec{Q}) d^+(2\vec{K} - \vec{P} + \vec{Q})) | d^+(\vec{P}) \rangle \rangle_{\omega}] - \frac{2\eta}{(\hbar\omega + i\delta)} \sum_{\vec{Q}} W_{\vec{Q}} \text{Sin} \left(\frac{[(\vec{P} - \vec{K}) \times \vec{Q}]_z L^2}{2} \right) \\
 & \quad \times \text{Sin} \left(\frac{[\vec{Q} \times \vec{K}]_z L^2}{2} \right) \times [e^{-i\varphi} \langle \langle (\hat{\rho}(\vec{P} - \vec{K} - \vec{Q}) d(\vec{Q} + \vec{K}) + d(\vec{Q} + \vec{K}) \hat{\rho}(\vec{P} - \vec{K} - \vec{Q})) | d^+(\vec{P}) \rangle \rangle_{\omega} \\
 & \quad - e^{i\varphi} \langle \langle (\hat{\rho}(\vec{P} - \vec{K} - \vec{Q}) d(\vec{K} - \vec{Q}) + d^+(\vec{K} - \vec{Q}) \hat{\rho}(\vec{P} - \vec{K} - \vec{Q})) | d^+(\vec{P}) \rangle \rangle_{\omega}] \quad (29)
 \end{aligned}$$

In the frame of the approximation (28) the two last sums in (29) happen to be equal to zero, due to the vorticity and symmetry properties of the system. But in other similar cases the different from zero

terms will appear. The truncations and the decouplings of the three-operator Green's functions generated by all four equations of motion (27) will be effectuated using the approximations

$$\begin{aligned}
 \left\langle \left\langle \frac{\hat{\rho}(\vec{P} - \vec{K} - \vec{Q} - \vec{R})}{\sqrt{N}} \hat{\rho}(\vec{R}) \hat{\rho}(\vec{Q}) \right| d^+(\vec{P}) \right\rangle \right\rangle_{\omega} & \approx G_{13}(\vec{P}, \omega) [\delta_{kr}(\vec{Q}, \vec{P} - \vec{K}) \langle \hat{\rho}(\vec{R}) \hat{\rho}(-\vec{R}) \rangle + (\delta_{kr}(\vec{R}, -\vec{Q}) \\
 & \quad + \delta_{kr}(\vec{R}, \vec{P} - \vec{K})) \langle \hat{\rho}(\vec{Q}) \hat{\rho}(-\vec{Q}) \rangle]; \\
 \left\langle \left\langle \frac{\hat{\rho}(\vec{P} - \vec{K} - \vec{Q})}{\sqrt{N}} \hat{\rho}(\vec{R}) \hat{\rho}(\vec{Q} - \vec{R}) \right| d^+(\vec{P}) \right\rangle \right\rangle_{\omega} & \approx G_{13}(\vec{P}, \omega) [\delta_{kr}(\vec{Q}, 0) \langle \hat{\rho}(\vec{R}) \hat{\rho}(-\vec{R}) \rangle + (\delta_{kr}(\vec{R}, \vec{P} - \vec{K}) + \delta_{kr}(\vec{R}, \vec{Q} + \vec{K} - \vec{P})) \langle \hat{\rho}(\vec{P} \\
 & \quad - \vec{K} - \vec{Q}) \hat{\rho}(\vec{Q} + \vec{K} - \vec{P}) \rangle]; \\
 \left\langle \left\langle \hat{\rho}(\vec{R}) \hat{\rho}(\vec{Q} - \vec{R}) \frac{\hat{D}(\vec{P} - \vec{K} - \vec{Q} - \vec{R})}{\sqrt{N}} \right| d^+(\vec{P}) \right\rangle \right\rangle_{\omega} & \approx \delta_{kr}(\vec{Q}, 0) G_{14}(\vec{P}, \omega) \langle \hat{\rho}(\vec{R}) \hat{\rho}(-\vec{R}) \rangle + G_{13}(\vec{P}, \omega) (\delta_{kr}(\vec{R}, \vec{P} - \vec{K}) \\
 & \quad + \delta_{kr}(\vec{R}, \vec{Q} + \vec{K} - \vec{P})) \langle \hat{\rho}(\vec{Q} + \vec{K} - \vec{P}) \hat{D}(\vec{P} - \vec{K} - \vec{Q}) \rangle];
 \end{aligned}$$

$$\left\langle \left\langle \hat{\rho}(\vec{R})\hat{\rho}(\vec{Q}) \frac{\hat{D}(\vec{P} - \vec{K} - \vec{Q} - \vec{R})}{\sqrt{N}} \left| d^+(\vec{P}) \right. \right\rangle \right\rangle_{\omega} \approx \delta_{kr}(\vec{R}, -\vec{Q})G_{14}(\vec{P}, \omega)\langle \hat{\rho}(\vec{Q})\hat{\rho}(-\vec{Q}) \rangle + G_{13}(\vec{P}, \omega)[\delta_{kr}(\vec{R}, \vec{P} - \vec{K})\langle \hat{\rho}(\vec{Q})\hat{D}(-\vec{Q}) \rangle + \delta_{kr}(\vec{Q}, \vec{P} - \vec{K})\langle \hat{\rho}(\vec{R})\hat{D}(-\vec{R}) \rangle]. \quad (30)$$

After the truncations and linearizations the multi-operator Green's functions are expressed through the one-operator Green's function $G_{1j}(\vec{P}, \omega)$, with $j = 1, 2, 3, 4$, and their four equations of motion can be written in a close form introducing the self-energy parts $\Sigma_{ij}(\vec{P}, \omega)$ as follows

$$\sum_{j=1}^4 G_{1j}(\vec{P}, \omega) \sum_{jk}(\vec{P}, \omega) = C_{1k}; \quad k = 1, 2, 3, 4 \quad (31)$$

There are 16 different components of the self energy part of the 4×4 matrix as follows

$$\begin{aligned} \Sigma_{11}(\vec{P}, \omega) &= (\hbar\omega + \bar{\mu} - E(\vec{P}) + i\delta) - 4 \sum_{\vec{Q}} W_{\vec{Q}}^2 \text{Sin}^2([\vec{P} \times \vec{Q}]_z I^2) \frac{\langle \hat{\rho}(\vec{Q})\hat{\rho}(-\vec{Q}) \rangle}{\hbar\omega + \bar{\mu} - E(\vec{P} - \vec{Q}) + i\delta} \\ &\quad - \frac{4\eta v(W_{\vec{P}-\vec{K}} N) \text{Sin}^2\left(\frac{[\vec{P} \times \vec{K}]_z I^2}{2}\right)}{\hbar\omega + \bar{\mu} - E(\vec{K}) + i\delta}; \\ \Sigma_{21}(\vec{P}, \omega) &= \frac{4\eta e^{2i\varphi} v(W_{\vec{P}-\vec{K}} N) \text{Sin}^2\left(\frac{[\vec{P} \times \vec{K}]_z I^2}{2}\right)}{\hbar\omega + \bar{\mu} - E(\vec{K}) + i\delta}; \\ \Sigma_{31}(\vec{P}, \omega) &= i\eta e^{i\varphi} \text{Sin}\left(\frac{[\vec{P} \times \vec{K}]_z I^2}{2}\right) \left(1 - \frac{2(W_{\vec{P}-\vec{K}} N)}{\hbar\omega + \bar{\mu} - E(\vec{K}) + i\delta}\right) \\ &\quad + \frac{4W_{\vec{P}-\vec{K}} \text{Sin}([\vec{P} \times \vec{K}]_z I^2)}{2} \hbar\omega + \bar{\mu} - E(\vec{K}) + i\delta \sum_{\vec{R}} W_{\vec{R}} \text{Sin}\left(\frac{[\vec{R} \times \vec{K}]_z I^2}{2}\right) \langle \hat{\rho}(\vec{Q})d(\vec{K} - \vec{R}) \rangle \sqrt{N} \\ &\quad + 4 \sum_{\vec{Q}} W_{\vec{Q}} W_{\vec{P}-\vec{K}} \text{Sin}\left(\frac{[\vec{P} \times \vec{Q}]_z I^2}{2}\right) \frac{\text{Sin}\left(\frac{[(\vec{P} - \vec{Q}) \times (\vec{P} - \vec{K})]_z I^2}{2}\right) \langle \hat{\rho}(\vec{Q})d(\vec{K} - \vec{Q}) \rangle \sqrt{N}}{\hbar\omega + \bar{\mu} - E(\vec{P} - \vec{Q}) + i\delta} \\ &\quad + 4 \sum_{\vec{Q}} W_{\vec{Q}} (W_{\vec{Q}+\vec{K}-\vec{P}}) W_{\vec{P}-\vec{K}} \text{Sin}\left(\frac{[\vec{P} \times \vec{Q}]_z I^2}{2}\right) \text{Sin}\left(\frac{[(\vec{P} - \vec{K}) \times \vec{Q}]_z I^2}{2}\right) \frac{\langle \hat{\rho}(\vec{Q} + \vec{K} - \vec{P})d(\vec{P} - \vec{Q}) \rangle \sqrt{N}}{\hbar\omega + \bar{\mu} - E(\vec{P} - \vec{Q}) + i\delta}; \\ \Sigma_{41}(\vec{P}, \omega) &= -\eta e^{i\sigma} \text{Cos}\left(\frac{[\vec{P} \times \vec{K}]_z I^2}{2}\right). \end{aligned} \quad (32)$$

These matrix elements form the first column of the 4×4 matrix $\|\Sigma_{ij}\|$. The second column is formed by

the matrix elements $\Sigma_{j2}(\vec{P}, \omega)$ with $j = 1, 2, 3, 4$ as follows

$$\begin{aligned} \Sigma_{12}(\vec{P}, \omega) &= 4\eta \frac{e^{-2i\varphi} v(W_{\vec{K}-\vec{P}} N) \text{Sin}^2\left(\frac{[\vec{P} \times \vec{K}]_z I^2}{2}\right)}{\hbar\omega + \bar{\mu} + E(\vec{K}) + i\delta}; \\ \Sigma_{22}(\vec{P}, \omega) &= \hbar\omega - \bar{\mu} + E(2\vec{K} - \vec{P}) + i\delta - 4 \sum_{\vec{Q}} W_{\vec{Q}}^2 \frac{\text{Sin}^2\left(\frac{[(2\vec{K} - \vec{P}) \times \vec{Q}]_z I^2}{2}\right) \langle \hat{\rho}(\vec{Q})\hat{\rho}(-\vec{Q}) \rangle}{\hbar\omega - \bar{\mu} + E(2\vec{K} - \vec{P} - \vec{Q}) + i\delta} \\ &\quad - 4\eta v \frac{(W_{\vec{P}-\vec{K}} N) \text{Sin}^2\left(\frac{[\vec{P} \times \vec{K}]_z I^2}{2}\right)}{\hbar\omega - \bar{\mu} + E(\vec{K}) + i\delta}; \end{aligned}$$

$$\begin{aligned} \Sigma_{32}(\vec{P}, \omega) &= i\eta e^{-i\varphi} \text{Sin}\left(\frac{[\vec{P} \times \vec{K}]_z I^2}{2}\right) \left[1 + \frac{2(W_{\vec{p}-\vec{k}} N)}{\hbar\omega - \bar{\mu} + E(\vec{K}) + i\delta} \right] \\ &\quad - 4 \frac{W_{\vec{p}-\vec{k}} \text{Sin}\left(\frac{[\vec{P} \times \vec{K}]_z I^2}{2}\right)}{\hbar\omega - \bar{\mu} + E(\vec{K}) + i\delta} \sum_{\vec{R}} W_{\vec{R}} \text{Sin}\left(\frac{[\vec{R} \times \vec{K}]_z I^2}{2}\right) \langle d^+(\vec{K} - \vec{R}) \hat{\rho}(-\vec{R}) \rangle \sqrt{N} \\ &\quad + 4 \sum_{\vec{Q}} W_{\vec{Q}} W_{\vec{K}-\vec{P}} \text{Sin}\left(\frac{[(2\vec{K} - \vec{P}) \times \vec{Q}]_z I^2}{2}\right) \text{Sin}\left(\frac{[(2\vec{K} - \vec{P} - \vec{Q}) \times (\vec{K} - \vec{P})]_z I^2}{2}\right) \frac{\langle d^+(\vec{K} - \vec{Q}) \hat{\rho}(-\vec{Q}) \rangle \sqrt{N}}{\hbar\omega - \bar{\mu} + E(2\vec{K} - \vec{P} - \vec{Q}) + i\delta} \\ &\quad + 4 \sum_{\vec{Q}} W_{\vec{Q}} (W_{\vec{p}-\vec{k}} - W_{\vec{p}-\vec{k}+\vec{Q}}) \times \text{Sin}\left(\frac{[(2\vec{K} - \vec{P}) \times \vec{Q}]_z I^2}{2}\right) \text{Sin}\left(\frac{[(\vec{P} - \vec{K}) \times \vec{Q}]_z I^2}{2}\right) \frac{\langle d^+(2\vec{K} - \vec{P} - \vec{Q}) \hat{\rho}(\vec{K} - \vec{P} - \vec{Q}) \rangle \sqrt{N}}{\hbar\omega - \bar{\mu} + E(2\vec{K} - \vec{P} - \vec{Q}) + i\delta}; \\ \Sigma_{42}(\vec{P}, \omega) &= \eta e^{-i\varphi} \text{Cos}\left(\frac{[\vec{P} \times \vec{K}]_z I^2}{2}\right). \end{aligned} \tag{33}$$

The third column of the 4×4 matrix $\|\Sigma_{ij}(\vec{P}, \omega)\|$ consists from the self-energy parts $\Sigma_{j3}(\vec{P}, \omega)$ with $j = 1, 2, 3, 4$ listed below

$$\begin{aligned} \Sigma_{13}(\vec{P}, \omega) &= 2i\eta e^{-i\varphi} \text{Sin}\left(\frac{[\vec{P} \times \vec{K}]_z I^2}{2}\right); \\ \Sigma_{23}(\vec{P}, \omega) &= 2i\eta e^{-i\varphi} \text{Sin}\left(\frac{[\vec{P} \times \vec{K}]_z I^2}{2}\right); \\ \Sigma_{33}(\vec{P}, \omega) &= (\hbar\omega + i\delta) \\ &\quad - \frac{4}{\hbar\omega + i\delta} \sum_{\vec{Q}} W_{\vec{Q}} \text{Sin}^2\left(\frac{[(\vec{P} - \vec{K}) \times \vec{Q}]_z I^2}{2}\right) \\ &\quad \times [(KW_{\vec{Q}} - W_{\vec{p}-\vec{k}}) \langle \hat{\rho}(\vec{Q}) \hat{\rho}(-\vec{Q}) \rangle \\ &\quad + (W_{\vec{p}-\vec{k}} - W_{\vec{p}-\vec{k}-\vec{Q}}) \langle \hat{\rho}(\vec{P} - \vec{K} - \vec{Q}) \hat{\rho}(\vec{K} + \vec{Q} - \vec{P}) \rangle]; \\ \Sigma_{43}(\vec{P}, \omega) &= 0. \end{aligned} \tag{34}$$

The fourth column is composed by the self-energy parts $\Sigma_{j4}(\vec{P}, \omega)$ with $j = 1, 2, 3, 4$. They are

$$\begin{aligned} \Sigma_{14}(\vec{P}, \omega) &= 2\eta e^{-i\varphi} \text{Cos}\left(\frac{[\vec{P} \times \vec{K}]_z I^2}{2}\right); \\ \Sigma_{24}(\vec{P}, \omega) &= -2\eta e^{i\varphi} \text{Cos}\left(\frac{[\vec{P} \times \vec{K}]_z I^2}{2}\right); \\ \Sigma_{34}(\vec{P}, \omega) &= \frac{4}{\hbar\omega + i\delta} \sum_{\vec{Q}} W_{\vec{Q}} W_{\vec{K}-\vec{P}+\vec{Q}} \text{Sin}^2\left(\frac{[(\vec{P} - \vec{K}) \times \vec{Q}]_z I^2}{2}\right) \\ &\quad \times \langle \hat{\rho}(\vec{Q} + \vec{K} - \vec{P}) \hat{D}(\vec{P} - \vec{K} - \vec{Q}) \rangle \end{aligned}$$

$$\begin{aligned} &+ \frac{4}{\hbar\omega + i\delta} \sum_{\vec{Q}} W_{\vec{Q}} W_{\vec{p}-\vec{k}} \text{Sin}^2\left(\frac{[(\vec{P} - \vec{K}) \times \vec{Q}]_z I^2}{2}\right) \\ &\quad \times [\langle \hat{\rho}(\vec{Q}) \hat{D}(-\vec{Q}) \rangle - \langle \hat{\rho}(\vec{Q} + \vec{K} - \vec{P}) \hat{D}(\vec{P} - \vec{K} - \vec{Q}) \rangle]; \\ \Sigma_{44}(\vec{P}, \omega) &= (\hbar\omega + i\delta) - \frac{4}{\hbar\omega + i\delta} \sum_{\vec{Q}} W_{\vec{Q}}^2 \\ &\quad \times \text{Sin}^2\left(\frac{[(\vec{P} - \vec{K}) \times \vec{Q}]_z I^2}{2}\right) \langle \hat{\rho}(\vec{Q}) \rho(-\vec{Q}) \rangle. \end{aligned} \tag{35}$$

The most of the self-energy parts $\Sigma_{ij}(\vec{P}, \omega)$ represented by the formulas (32)–(35) contain the average values of the two-operator products. They were calculated using the ground state wave function $|\psi_g(k)\rangle$ (11) and have the expressions

$$\begin{aligned} \langle \psi_g(k) | \hat{\rho}(\vec{Q}) \hat{\rho}(-\vec{Q}) | \psi_g(k) \rangle &= 4u^2 v^2 N \text{Sin}^2\left(\frac{[\vec{K} \times \vec{Q}]_z I^2}{2}\right); \\ \langle \psi_g(k) | \hat{\rho}(\vec{Q} + \vec{P} - \vec{K}) \hat{\rho}(\vec{K} - \vec{P} - \vec{Q}) | \psi_g(k) \rangle \\ &= 4u^2 v^2 N \text{Sin}^2\left(\frac{[\vec{K} \times (\vec{P} + \vec{Q})]_z I^2}{2}\right); \\ \langle \psi_g(k) | \hat{\rho}(\vec{Q} + \vec{P} - \vec{K}) \hat{\rho}(\vec{K} - \vec{P} - \vec{Q}) | \psi_g(k) \rangle \\ &= 4u^2 v^2 \bar{N} \text{Sin}^2\left(\frac{[\vec{K} \times (\vec{P} + \vec{Q})]_z I^2}{2}\right); \\ \langle \psi_g(k) | \hat{\rho}(\vec{Q}) \hat{D}(-\vec{Q}) | \psi_g(k) \rangle &= 2iu^2 v^2 N \text{Sin}\left(\frac{[\vec{K} \times \vec{Q}]_z I^2}{1}\right); \\ \langle \psi_g(k) | \hat{\rho}(\vec{Q} + \vec{P} - \vec{K}) \hat{\rho}(\vec{K} - \vec{P} - \vec{Q}) | \psi_g(k) \rangle \\ &= 2iu^2 v^2 \bar{N} \text{Sin}\left(\frac{[\vec{K} \times (\vec{P} + \vec{Q})]_z I^2}{1}\right); \end{aligned}$$

$$\begin{aligned}
& \langle \psi_g(k) | d^\dagger(\vec{K} - \vec{Q}) \hat{\rho}(-\vec{Q}) | \psi_g(k) \rangle \sqrt{N} \\
& \quad = 21uv^3 \bar{N} \text{Sin}\left(\frac{[\vec{K} \times (\vec{Q} - \vec{Q})]_z l^2}{2}\right); \\
& \langle \psi_g(k) | d^\dagger(\vec{P} - \vec{Q}) \hat{\rho}(\vec{P} - \vec{Q} - \vec{K}) | \psi_g(k) \rangle \sqrt{N} = \\
& \quad - 2iuv^3 N \text{Sin}\left(\frac{[\vec{K} \times (\vec{P} - \vec{Q})]_z l^2}{2}\right); \\
& \langle \psi_g(k) | \hat{\rho}(\vec{Q}) d(\vec{K} - \vec{Q}) | \psi_g(k) \rangle \sqrt{N} = \\
& \quad - 2iuv^3 N \text{Sin}\left(\frac{[\vec{K} \times \vec{Q}]_z l^2}{2}\right); \\
& \langle \psi_g(k) | \hat{\rho}(\vec{P} + \vec{Q}) d(\vec{K} - \vec{P} - \vec{Q}) | \psi_g(k) \rangle \sqrt{N} = \\
& \quad - 2iuv^3 N \text{Sin}\left(\frac{[\vec{K} \times (\vec{P} + \vec{Q})]_z l^2}{2}\right). \quad (36)
\end{aligned}$$

All these averages are extensive values proportional to N , they essentially depend on the wave vectors and on the small parameters of the types u^2v^2 or uv^3 .

But only the averages of the type $\langle \hat{\rho}(\vec{Q}) \hat{\rho}(-\vec{Q}) \rangle$ are real, positive with a constant sign at any values of the wave vectors.

All another averages are pure imaginary changing their signs in dependence on their arguments leading to small absolute values of the corresponding self-energy parts. All of them will be dropped to simplify the cumbersome expressions (32)–(35).

In spite of the made approximations concerning the many operator Green's functions and the averages of the two-operator products, the obtained self-energy parts remain cumbersome. But there is one possibility to radically simplify the further calculations. It is related with the collinear geometry of the experimental observation of the elementary excitations, when their propagation direction coincide or is exactly opposite with the condensate wave vector \vec{k} . This geometry will be discussed below.

The cumbersome dispersion equation is expressed in general form by the determinant equation

$$\det|\sum_{ij}(\vec{P}, \omega)| = 0; \vec{P} = \vec{K} + \vec{q}. \quad (37)$$

It can be essentially simplified in collinear geometry, when the wave vectors \vec{P} of the elementary excitations are parallel or antiparallel to the Bose-Einstein condensate wave vector \vec{k} . We will repre-

sent the wave vectors \vec{P} in the form $\vec{P} = \vec{k} + \vec{q}$, accounting them from the condensate wave vector \vec{k} . The relative wave vector \vec{Q} will be also collinear to \vec{k} . In this case the projections of the wave vector products $[\vec{P} \times \vec{K}]_z$ as well as all coefficients proportional to $\text{Sin}([\vec{P} \times \vec{K}]_z l^2 / 2)$ and a half of the matrix elements $\sum_{ij}(\vec{P}, \omega)$ in the Eq. (37) vanish. The determinant Eq. (37) disintegrates in two independent equations. One of them concerns only to optical plasmons and has a simple form

$$\sum_{33}(\vec{K} + \vec{q}; \omega) = 0; [\vec{q} \times \vec{K}]_z = 0 \quad (38)$$

whereas the second equation contains only the diagonal self-energy parts \sum_{11} , \sum_{22} , \sum_{44} , and the quasi-average constant η

$$\begin{aligned}
& \sum_{11}(\vec{K} + \vec{q}, \omega) \sum_{22}(\vec{K} + \vec{q}, \omega) \sum_{44}(\vec{K} + \vec{q}, \omega) \\
& \quad - 2\eta^2 (\sum_{11}(\vec{K} + \vec{q}, \omega) + \sum_{22}(\vec{K} + \vec{q}, \omega)) = 0 \quad (39)
\end{aligned}$$

It determines three interconnected branches. Two of them describe the proper collective excitations of Bose-Einstein condensed magnetoexcitons and the third branch concerns the acoustical plasmons. In spite of the collinear condition $[\vec{q} \times \vec{K}]_z = 0$, the Eqs. (38) and (39) and their energy spectra $\omega(\vec{q})$ are not invariant under the inversion operation when \vec{q} is substituted by $-\vec{q}$, because in the system does exist a well defined direction selected by the wave vector \vec{k} . For this reason the elementary excitations with wave vector \vec{q} and $-\vec{q}$ have different energies.

The solutions of the dispersion Eq. (39) will be discussed in two limiting cases. One of them is the point $k = 0$, where the system behaves as an ideal Bose gas and another case of considerable values of wave vectors $kl \approx 3 - 4$, when the Bose-Einstein condensed 2D magnetoexcitons can exist in a form of metastable dielectric liquid phase or of dielectric droplets. But in all cases the average value $\langle \hat{\rho}(\vec{Q}) \hat{\rho}(-\vec{Q}) \rangle$ and other similar expressions are determined in HFBA by the formulas (36). They are characterized by a coherence factor $\text{Sin}^2([\vec{K} \times \vec{Q}]_z l^2 / 2)$, which vanishes in the point $k = 0$. All contributions to the self-energy parts proportional to square of Coulomb interaction matrix elements W_Q^2 multiplied by the averages $\hat{\rho}(\vec{Q}) \hat{\rho}(-\vec{Q})$ vanish also making a 2D magnetoexciton system a pure ideal gas, when the influence of the excited Landau levels is neglected. This unusual result was revealed for the first time by Lerner and Lozovik [15–17] and was confirmed by Paquet et al. [19]. In

the case $k = 0$ because the vanishing of the averages (36) the self-energy parts become

$$\begin{aligned}\sigma_{11}(\vec{P}, \omega) &= \hbar\omega + \bar{\mu} - E(P); \\ \sigma_{22}(\vec{P}, \omega) &= \hbar\omega - \bar{\mu} + E(-P); \\ \sigma_{44}(\vec{P}, \omega) &= \hbar\omega\end{aligned}\quad (40)$$

and the excitonic part of the dispersion relation as well the acoustic plasmon frequency look as

$$\begin{aligned}\hbar\omega_{\text{ex}}(P) &= \pm \sqrt{(\bar{\mu} - E(P))^2 + 4\eta^2}; \\ \hbar\omega_A(P) &= 0.\end{aligned}\quad (41)$$

The values $\bar{\mu} = E(k)(1 - 2y^2)$ and $\eta = (E(k) - \bar{\mu})y = E(k)y^3$ in the point $k = 0$ turn to vanish, i.e., $\bar{\mu} = \eta = E(0) = 0$, what leads to the free magnetoexciton dispersion law $\hbar\omega_{\text{ex}}(P) = \pm E(P)$, and coincides with the result obtained earlier in Ref. [19]. The acoustical plasmon branch as well as the optical branch has frequencies equal to zero. The case $k \neq 0$, but $v = 0$, can be obtained from the previous formula because, as earlier, the averages (36) as well as the parameter η are vanishing, whereas the chemical potential is different from zero, i.e., $\bar{\mu} = E(k)$.

In this case, the exciton dispersion law in collinear geometry with $P = k + q\text{Cos}\alpha$ has the form

$$\begin{aligned}\hbar\omega_{\text{ex}}(q) &= \pm (E(k + q\text{Cos}\alpha) - E(k)), \\ \text{Cos}\alpha &= \pm 1, q > 0\end{aligned}\quad (42)$$

The both dependences are represented in Figure 2, where $x = ql$ was introduced.

The case of $k \neq 0$ with filling factor $v = v^2 < 1$ represents interest because in this region of parameters a metastable dielectric liquid phase does exist. It is formed by the Bose–Einstein condensed magnetoexcitons with $kl \approx 3 - 4$ and with different from zero motional dipole moments $\vec{\rho} = [k \times \vec{z}]l^2$. This state was revealed in Ref. [20] considering the system of electrons and holes on their lowest Landau levels, without addressing to excited Landau levels (ELLs), but taking into account coherent excited states, when one e-h pair exits from the condensate leaving all another pairs in their coherent pairing state.

The correlation energy was calculated beyond the Hartree–Fock–Bogoliubov approximation (HFBA) in the frame of Keldysh–Kozlov–Kopaev method using the Nozieres Comte approach [20, 41].

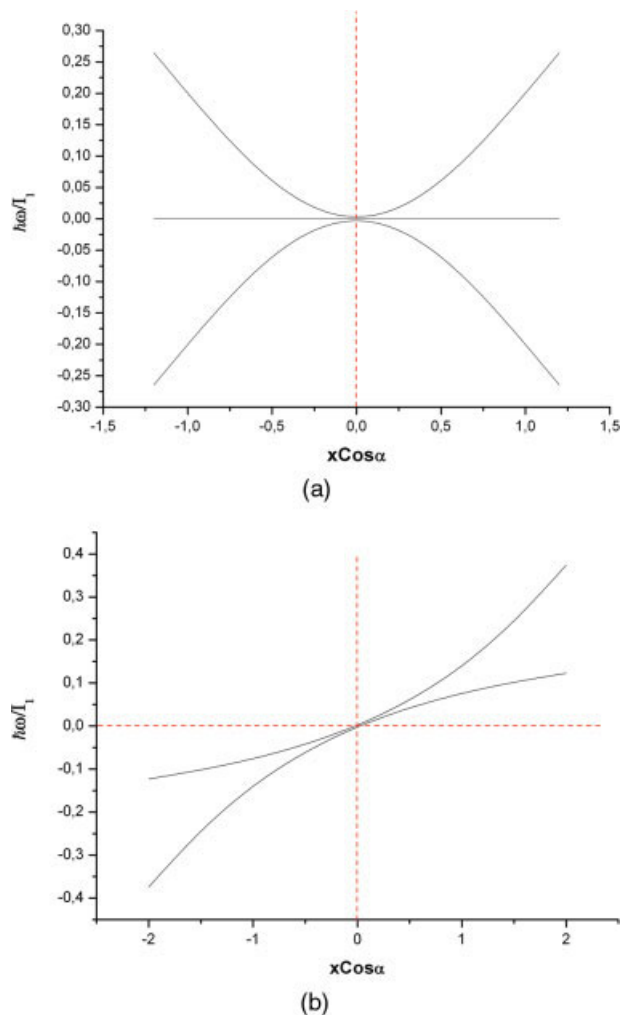


FIGURE 2. The energy spectrum of elementary excitations of magnetoexcitons and acoustical plasmons in the case when concentrations corrections have not been taken into account. (a) The wave vector of BEC magnetoexcitons equal to 0. (b) The wave vector k is different from zero, but the filling factor equals to zero. [Color figure can be viewed in the online issue, which is available at www.interscience.wiley.com.]

The Bose–Einstein condensed magnetoexcitons moving as a whole with wave vector \vec{k} and with parallel motional dipole moments $\vec{\rho}$ have a significant polarizability which gives rise to attractive interaction between them and lower on the energy scale the values of the chemical potential and of the mean energy per one e-h pair. But this lowering is not monotonous and at some value of the filling factor v_m^2 the relative minimum on the corresponding curves appear with positive compressibilities in their vicinity. The relative minimum on the chemi-

cal potential curve depends essentially on the damping of magnetoexciton level. It was investigated in the Ref. [21] and is represented in Figure 3.

If the average filling factor ν^2 is less than ν_m^2 the dielectric liquid phase will exist in the form of droplets with optimal concentration inside them $n_{ex}/2\pi l_0^2$ corresponding to filling factor ν_m^2 .

The collective elementary excitations are calculated in the conditions $K \approx 3 - 4$ and $\nu^2 \approx \nu_m^2$, when the ground state of the magnetoexcitons is similar with the metastable dielectric liquid phase.

Even in collinear geometry the diagonal self-energy parts $\Sigma_{ii}(\vec{K} + \vec{q}, \omega)$ with $i = 1, 2, 3, 4$ and $kl = 3, 6$ can not be calculated analytically at arbitrary values of the relative wave vector \vec{q} . By this reason we will obtain the analytical expressions in the case $kl \approx 3, 6$ and $ql \leq 1 < kl$ using a series expansions on the small values $ql < 1$ as compared with $kl \approx 3, 6$.

Up till now we have discussed the energy spectrum of a Bose–Einstein condensed magnetoexcitons in pure ideal conditions which take place in the case $k = 0$, when the interactions in the electron-hole system are reciprocally compensated at arbitrary values of the filling factor $\nu^2 \neq 0$, as well as in the case $k \neq 0$, when the nonlinearity is completely neglected putting $\nu = 0$. In the last case taking into account the nonlinearity $\nu^2 \neq 0$ we can observe its unusual influence on the earlier discussed energy spectrum leading to its qualitative new and principal changes. They are different from the simple additions of the concentration corrections to the exciton branches of spectrum as one could expect on the base of a simple perturbation theory. Instead of it the influence of the concentration terms proportional to $u^2 \nu^2$ entering into the compositions of

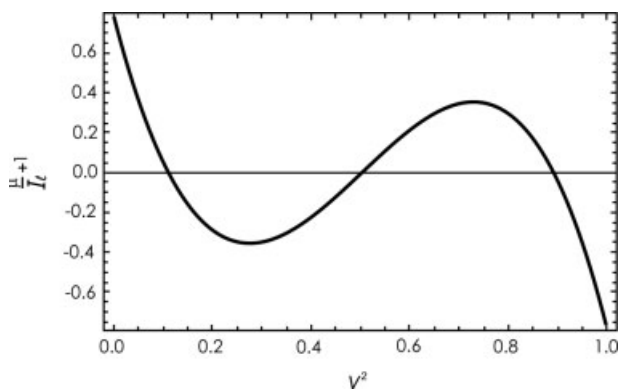


FIGURE 3. The relative minimum on the chemical potential dependence on the filling factor.

the self-energy parts σ_{11} , σ_{22} , and σ_{44} happens to be much more important. The self-energy parts contain the different linear on $\tilde{\omega}$ expressions of the type $L_i(\tilde{\omega}) = \tilde{\omega} + \tilde{\mu} - \tilde{E}(y + x\text{Cos}\alpha)$ which appear in the forms $A_i/L_i(\tilde{\omega})$ and determine the concentration corrections. For simplicity we will demonstrate their influence taking into account only the denominators in the first power. The self-energy parts σ_{11} and σ_{22} contain also such denominators in power two of the forms $B_i/(L_i(\tilde{\omega}))^2$, but these terms for simplicity were neglected in the numerical calculations. The presence of the unknown frequency $\tilde{\omega}$ in the denominators side by side with another term in numerators leads to the increasing of the order of the dispersion equation and of the number of the energy spectrum branches. In our concrete case the order of dispersion equation is doubled and instead of three branches of the energy spectrum we are dealing with six branches. Two of them are acoustical plasmon branches with energies proportional to the perturbation theory parameter $\nu^2(1 - \nu^2)$ and with different \pm signs. It was natural to expect the appearance of these two branches of acoustical plasmon spectrum and the same takes place with the optical plasmon spectrum. Unusual behavior happens with the exciton energy and quasienergy branches which become doubled undergoing each of them a bifurcation. The new branches have the form of the previous exciton branch plus or minus one additional of amount approximately equal to the energy of the acoustical plasmon with wave vector different from the wave vector of the exciton elementary excitation by the condensate wave vector k . The same change takes place with the quasienergy exciton branch. The neglected denominator in power two could create exciton branch with two acoustical plasmons. The Bose–Einstein condensation with $k \neq 0$ means that the e-h system is moving as regards the laboratory reference frame with a velocity equal to the group velocity V_g of the magnetoexcitons, reflected in the Figure 4. It means that the terms $\hbar \vec{V}_g \vec{q}$ will appear in the dispersion relations for all three branches. To create the exciton-type collective elementary excitations when the ground state of the system is a dielectric liquid phase with negative values of the chemical potential μ it is necessary to liberate an exciton from the liquid communicating it an amount of energy at least equal to $|\mu|$. This values $|\mu|$ are equal to $0.31I_l$ and $0.69I_l$ at the filling factors ν^2 equal to 0.028 and 0.28 correspondingly. Because the concentration corrections to the energy spectrum in our case appear in the form of acoustical plasmon energy $\hbar\omega_{AP}$

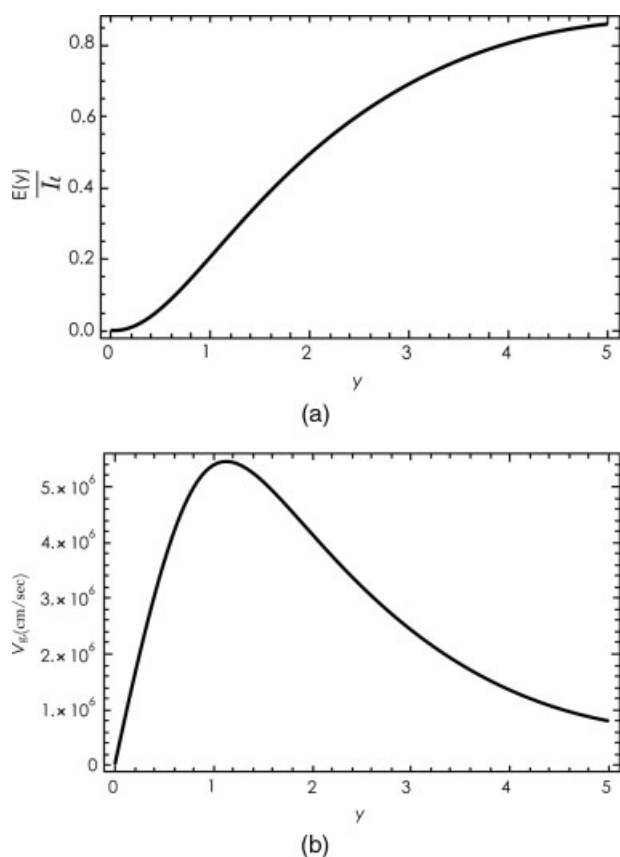


FIGURE 4. (a) The dispersion law of the magnetoexciton. (b) The group velocity $V_g(k)$ of the magnetoexciton.

two exciton branches have approximately the energies $|\mu| \pm \hbar\omega_{AP}$. The exciton and plasmon quasi-energy branches can be obtained from the exciton and plasmon energy branches by two successive reflections as regards two coordinate axes. These properties can be observed on the Figure 5.

4. Conclusion

The combined two-dimensional magnetoexciton-cyclotron resonance was described as a dipole-active transition in the frame of the second order perturbation theory, when the electron-radiation and electron-electron Coulomb interactions are used as perturbations. This combined optical quantum transition can be described also in the frame of the first-order perturbation theory as a quadrupole active quantum transition with a probability proportional to $|\tilde{Q}_{2D}|^2$, which vanishes in the Faraday geometry of excitation. The Hamiltonian describing

the interaction of the circularly polarized radiation with the 2D electron-heavy-hole system in a strong perpendicular magnetic field was deduced. The magnetoexcitons and the heavy holes are characterized supplementary by their quantum states in the frame of the p -type valence band with strong spin-orbital coupling. The p -functions of the type $(x \pm iy)$ are characterized by the orbital momentum projection $M = \pm 1$ on the direction of the external magnetic field, what is equivalent to introduction of the circular polarization vectors $\vec{\sigma}_M = 1/\sqrt{2}(\vec{a}_1 \pm i\vec{a}_2)$, where \vec{a}_1 and \vec{a}_2 are in-plane unit vectors. The value M or $\vec{\sigma}_M$ are supplementary characteristic of the magnetoexcitons side-by-side with the quantum numbers n_e and n_h of the Landau levels and with the exciton wave vector \vec{k}_{ex} .

The circularly polarized radiation consists of photons with wave vectors \vec{Q} and polarization vectors $\vec{\sigma}_Q^\pm$, which are arbitrary oriented in the 3D space. The photons interact with e-h pairs situated on the 2D layer in a strong perpendicular magnetic field. They are characterized by their circular polarization vectors $\vec{\sigma}_M$. The light-matter interaction is characterized by the matrix elements proportional to the scalar products $(\vec{\sigma}_Q^\pm \cdot \vec{\sigma}_M)$. The creation of the e-h pair in the presence of a background electron gives rise to the new combined exciton-electron absorption bands. When the new optically created electron has the same spin orientation along the

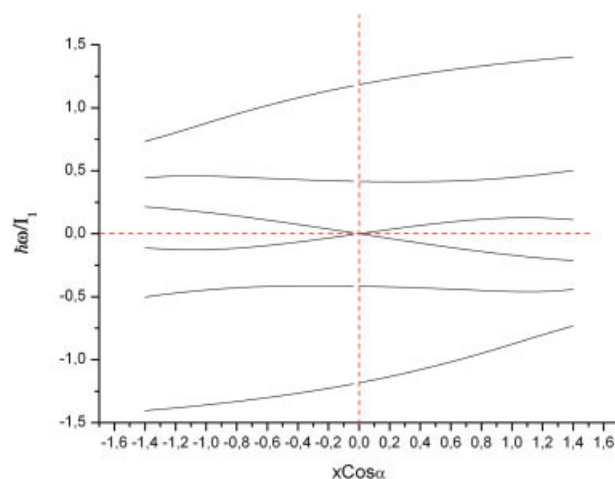


FIGURE 5. The energy spectrum of elementary excitations of magnetoexcitons and acoustical plasmons in the case when filling factor of the lowest Landau levels equals to $\nu^2 = 0.28$. The dimensionless wave vector of the Bose–Einstein condensed magnetoexcitons equals to 3, 6. [Color figure can be viewed in the online issue, which is available at www.interscience.wiley.com.]

magnetic field direction as the background electron, both electrons take identical part in the quantum transitions as in the initial stage as well as in the final stage with the contribution of the direct and exchange Coulomb interaction terms. For another circular polarization of the light both electrons have antiparallel spins and contribution of the exchange interaction terms is absent. As a result the probabilities of the combined quantum transitions in the first case contain a supplementary factor 4 as compared to the second variant.

The band shapes are determined by the spectral functions $f_1(\tilde{\Delta})$ and $f_2(\tilde{\Delta})$ and by the resonant denominators of the second-order perturbation theory. The spectral functions are also different for different circular polarizations because the exchange Coulomb interaction contributes only to the first one. The absorption band shapes in the Faraday geometry were obtained. Both spectral functions $f_1(\tilde{\Delta})$ and $f_2(\tilde{\Delta})$ have a maximal width equal to the ionization potential of the magnetoexciton at the point $k = 0$.

The density of states in 2D structures leads to spectral functions $f_i(\tilde{\Delta})$, $i = 1, 2$ with maximal values at the point $\tilde{\Delta} = -1$, which corresponds to the creation of magnetoexcitons at the bottom of their energy band. In this region both spectral functions decrease linearly with a smaller slope in the case $f_1(\tilde{\Delta})$ and with a larger slope in the case $f_2(\tilde{\Delta})$. Near the upper limit of the variable $\tilde{\Delta} = 0$ the function $f_1(\tilde{\Delta})$ decreases linearly whereas the function $f_2(\tilde{\Delta})$ decreases exponentially. The influence of the resonant denominators on the absorption band shapes is especially important in the region of not so high magnetic field strength when the electron cyclotron energy is comparable with the magnetoexciton ionization energy. The resultant band shapes are characterized by the decreasing heights and by increasing widths when the magnetic field increases. The widths are due to inhomogeneous broadening arising from the magnetoexciton energy band dispersion law. The two absorption band shapes corresponding to different circular polarizations in the Faraday geometry can be distinguished experimentally.

The circularly polarized light creates the spin-polarized electrons, leads to optical alignment of magnetoexcitons and induces the nuclear magnetic field generation through the Fermi contact hyperfine interaction. Its influence on the Zeeman splitting of the magnetoexciton levels can be observed as the Overhauser effect.

The collective elementary excitations of a system of Bose-Einstein condensed magnetoexcitons interacting

with electron-hole plasma in a strong perpendicular magnetic field were studied. The breaking of the gauge symmetry was introduced into the Hamiltonian following the Bogoliubov's theory of quasiaverages. The equations of motion for integral two-particle operators describing the creation and annihilation of magnetoexcitons as well as the electron-hole plasma density fluctuations were derived. The two-particle operators were used to construct four types of Green's functions. Two of them are normal and abnormal exciton Green's functions whereas another two describe the acoustical and optical plasmons. The Green's functions obey to four equations of motion, which contain nonlinearity and higher order Green's functions, for which another more complicate equations of motion were obtained. The chains of equations of motion containing the six-particle Green's functions were truncated expressing approximately the six-particle Green's functions through the two-particle Green's functions multiplied by the average values of the four-particle operators. This disconnection procedure permits to obtain an enclosed set of four Dyson equations with self-energy parts Σ_{ij} with $i, j = 1, 2, 3, 4$ forming a 4×4 matrix. Its determinant gives rise to four order dispersion equation, the elements of which are the self-energy parts. In collinear geometry of observation when the elementary excitation wave vectors are collinear with the condensate wave vector the dispersion equation desintegrates in two independent equations. One of them contains only the self-energy part of the optical plasmons, whereas the second third order dispersion equation contains the diagonal self-energy parts of other three components. In their compositions there are denominators containing the unknown frequency what doubled the order of the dispersion equation transforming it from three to six orders. Six branches of the energy spectrum describe two exciton-plasmon energy branches, two exciton-plasmon quasienergy branches and two of them with \pm signs belong to acoustical plasmon branches.

References

1. Liberman, M. A.; Johanson, B. *Uspekhi Fiz Nauk* 1995, 165, 121.
2. Lai, D. *Rev Mod Phys* 2001, 73, 629.
3. Stormer, H. L. *Rev Mod Phys* 1999, 71, 875.
4. Das Sarma, S.; Pinczuk, A., Eds. *Perspectives in Quantum Hall Effects*; Wiley: New York, 1997.
5. Rashba, E. I. *Pure Appl Chem* 1995, 67, 409.
6. Tsui, D. C.; Stormer, H. L.; Gossard, A. C. *Phys Rev Lett* 1982, 8, 1559.

7. Laughlin, R. B. *Phys Rev Lett* 1983, 50, 13.
8. MacDonald, A. H.; Rezayi, E. H.; Keller, D. *Phys Rev Lett* 1992, 68, 1939.
9. Haldane, F. D. M. *Phys Rev Lett* 1983, 51, 605.
10. Halperin, B. I. *Phys Rev Lett* 1984, 52, 1583.
11. Jain, J. K. *Phys Rev Lett* 1989, 63, 199.
12. Arovas, D.; Schriffer, J. R.; Wilczek, F. *Phys Rev Lett* 1984, 53, 722.
13. Girvin, S. M.; MacDonald, A. H.; Platzman, P. M. *Phys Rev B* 1986, 33, 2481.
14. Haldane, F. G. H.; Rezayi, E. H. *Phys Rev Lett* 1985, 54, 359.
15. Lerner, I. V.; Lozovik, Y. E. *Zh Eksp Teor Fiz* 1980, 78, 1167.
16. Lerner, I. V.; Lozovik, Y. E. *J Low Temp Phys* 1980, 38, 333.
17. Lerner, I. V.; Lozovik, Y. E. *Zh Eksp Teor Fiz* 1981, 80, 1488 [*Sov Phys JETP* 1981, 53, 763].
18. (a) Dzyubenko, A. B.; Lozovik, Y. E. *Fiz Tverd Tela (Leningrad)* 1983, 25, 1519; (b) Dzyubenko, A. B.; Lozovik, Y. E. *Fiz Tverd Tela (Leningrad)* 1984, 26, 1540; (c) Dzyubenko, A. B.; Lozovik, Y. E. *Sov Phys Solid State* 1983, 25, 874; (d) Dzyubenko, A. B.; Lozovik, Y. E. *Sov Phys Solid State* 1984, 26, 938; (e) Dzyubenko, A. B.; Lozovik, Y. E. *J Phys A* 1991, 24, 415.
19. (a) Paquet, D.; Rice, T. M.; Ueda, K. *Phys Rev B* 1985, 32, 5208; (b) Rice, T. M.; Paquet, D.; Ueda, K. *Helv Phys Acta* 1985, 58, 410.
20. Moskalenko, S. A.; Liberman, M. A.; Snoke, D. W.; Botan, V. *Phys Rev B* 2002, 66, 245316.
21. (a) Moskalenko, S. A.; Liberman, M. A.; Snoke, D. W.; Botan, V.; Johansson, B. *Physica E* 2003, 19, 278; (b) Botan, V.; Liberman, M. A.; Moskalenko, S. A.; Snoke, D. W.; Johansson, B. *Physica B* 2004, 346–347 C, 460.
22. Moskalenko, S. A.; Liberman, M. A.; Khadzhi, P. I.; Dumanov, E. V.; Podlesny, I. V.; Botan, V. *Solid State Commun* 2006, 140, 236.
23. (a) Apalkov, V. M.; Rashba, E. I. *Phys Rev B* 1992, 46, 1628; (b) Apalkov, V. M.; Rashba, E. I. *Phys Rev B* 1993, 48, 18312; (c) Apalkov, V. M.; Rashba, E. I. *Pisma Zh Eksp Teor Fiz* 1991, 54, 160; (d) Apalkov, V. M.; Rashba, E. I. *Pisma Zh Eksp Teor Fiz* 1992, 55, 38.
24. Chen, X. M.; Quinn, J. J. *Phys Rev Lett* 1993, 70, 2130.
25. Griffin, A.; Snoke, D. W.; Stringari, S., Eds. *Bose-Einstein Condensation*; Cambridge University Press: Cambridge, 1995.
26. Butov, L. V.; Ivanov, A. L.; Imamoglu, A.; Littlewood, P. B.; Shashkin, A. A.; Dolgoplov, V. T.; Campman, K. L.; Gosard, A. C. *Phys Rev Lett* 2001, 86, 5608.
27. Keldysh, L. V.; Kozlov, A. N. *Zh Eksp Teor Fiz* 1968, 54, 978 [*Sov Phys JETP* 1968, 27, 52].
28. Bar-Joseph, I. *Semicond Sci Technol* 2005, 20, R29.
29. Finkelstein, G.; Shtrikman, H.; Bar-Joseph, I. *Phys Rev Lett* 1995, 74, 976.
30. Yakovlev, D. R.; Kochereshko, V. P.; Suris, R. A.; Schenk, H.; Ossau, W.; Waag, A.; Landwehr, G.; Christianen, P. C. M.; Maan, J. C. *Phys Rev Lett* 1997, 79, 3974.
31. Kochereshko, V. P.; Yakovlev, D. R.; Suris, R. A.; Astakhov, G. V.; Faschinger, W.; Ossau, W.; Landwehr, G.; Wojtowicz, T.; Karczewski, G.; Kossut, J. *Optical Properties of 2D Systems with Interacting Electrons*; Ossau, W. J., Suris, W., Eds.; NATO Science Series II: Mathematics, Physics and Chemistry, Vol. 119; Kluwer Academic Publishers: Dordrecht, Boston, London, 2003, p 125.
32. Dzyubenko, A. B. *Phys Rev B* 2001, 64, 241101(R).
33. Dzyubenko, A. B.; Sivachenko, A. Y. *Phys Rev Lett* 2000, 84, 4429.
34. Moskalenko, S. A.; Liberman, M. A.; Khadzhi, P. I.; Dumanov, E. V.; Podlesny, I. V.; Botan, V. V. *Physica E* 2007, 39, 137.
35. Moskalenko, S. A.; Liberman, M. A.; Podlesny, I. V. *Phys Rev B* 2009, 79, 125425.
36. Abramowitz, M.; Stegun, I. A. *Handbook of Mathematical Functions*; Courier Dover: New York, 1972; 1046 p.
37. Gor'kov, L. P.; Dzyaloshinskii, I. E. *Zh Eksp Teor Fiz* 1967, 53, 717. [*Sov Phys JETP* 1968, 26, 449].
38. Pines, D. *Elementary Excitations in Solids*; Benjamin: New York, 1963.
39. Abrikosov, A. A.; Gor'kov, L. P.; Dzyaloshinskii, I. E. *Methods of Quantum Field Theory in Statistical Physics*; Dover: New York, 1975.
40. Zubarev, D. N. *Sov Phys Uspekhi Fiz Nauk* 1960, 71, 71.
41. Moskalenko, S. A.; Snoke, D. W. *Bose-Einstein Condensation of Excitons and Biexcitons and Coherent Nonlinear Optics with Excitons*; Cambridge University Press: Cambridge, 2000; 415 p.